NISTIR 5682

STRENGTHENING METHODOLOGY FOR LIGHTLY REINFORCED CONCRETE FRAMES: RECOMMENDED DESIGN GUIDELINES FOR STRENGTHENING WITH INFILL WALLS

Long T. Phan
Geraldine S. Cheok
Diana R. Todd

July 1995
Building and Fire Research Laboratory
National Institute of Standards and Technology
Gaithersburg, MD 20899

U.S. Department of Commerce
Ronald H. Brown, *Secretary*
Technology Administration
Mary L. Good, *Under Secretary for Technology*
National Institute of Standards and Technology
Arati Prabhakar, *Director*

ABSTRACT

A study of the sensitivity of the behavior of lightly reinforced concrete frames strengthened using the infill wall method to certain variables was conducted. These variables include the infill wall type (cast-in-place and precast), wall thickness, and the amount of anchor area and anchor type. The hysteretic behavior of the frames were predicted using three parameters and equations proposed in previous NIST work. Both quasi-static and transient dynamic analyses were performed using the program IDARC. General design guidelines are proposed based on these analyses and on observations gathered from existing experimental tests.

Keywords: Building technology, concrete, dynamic analysis, frames, infill wall, lightly reinforced, quasi-static analysis, seismic strengthening.

TABLE OF CONTENTS

LIST OF TABLES

LIST OF FIGURES

1.0 INTRODUCTION

1.1 GENERAL

In the past two decades, it has been recognized by the researchers and design engineers that a large percentage of the existing reinforced concrete (RC) buildings in the United States are inadequate for resisting cyclic lateral loads imposed on them in the event of an earthquake. These are concrete frame buildings that were designed primarily for gravity loads and built mostly prior to the 1970s in the mid-western and eastern regions of the United States. Most of these buildings are typically less than five stories in height and have characteristic reinforcement details that were acceptable based on the building codes and standards used at the time they were designed and constructed. However, they have since been identified by experimental studies and by failures in past earthquakes as inadequate for seismically induced loads. These buildings, for which include typical reinforcement details of (1) low longitudinal reinforcement ratios for columns, (2) little or no transverse reinforcement within the beam-column joint regions, and (3) large spacing between column transverse reinforcement which results in little confinement of the concrete core, are commonly categorized as lightly reinforced concrete (LRC) construction. Catastrophic structural failures that occurred in the 1971 San Fernando, 1985 Mexico City, and 1988 Armenia earthquakes, among others, illustrate the vulnerability and the potential for large loss of life in these LRC buildings.

Development of techniques or methodologies for seismic strengthening of these LRC buildings has been the focus of much research in recent years. As a result, many research projects on seismic strengthening of LRC buildings, most of which were experimental, have been conducted. In most of these programs, cyclic lateral load tests were performed on scaled specimens which modeled the subassemblages (one-bay, one-story frames, beam-column joints, or columns) of the LRC buildings. From each test program, conclusions have been drawn concerning the merits of the strengthening technique used. These studies revealed, in a qualitative sense, the effectiveness of various strengthening techniques and the problems associated with the techniques. However, because experimental work is often costly, none of the test programs had a broad enough scope to include all possible factors which may influence the seismic performance of the frame before and after strengthening.

A review of published literature showed that the four most common strengthening techniques, which have been experimentally proven to increase either the lateral strength capacity or the ductility of LRC buildings, are:

- **The infill wall technique** (See Phan, et. al. [1993, 1994] for references) involves filling the existing openings in RC frames with either cast-in-place (CIP) concrete walls (connected to the existing construction with epoxied or wedge anchor dowels, and/or shear keys), single or multiple precast concrete wall panels (connected by welding to new steel anchors in the original construction), or masonry walls (either brick or concrete blocks). The newly added rigid infill walls act primarily as shear walls and reduce the shear demand on the existing frame.

- **The beam-column joint upgrading technique** seeks to improve seismic performance of the joint mainly in terms of improved ductility by attaching external reinforcement such as bolted steel plates or angles to the joint region. Although many experimental studies of the behavior of typical interior and exterior joints under cyclic loads have been conducted to date (See Phan, et. al. [1993, 1994] for references), there has been very little experimental testing of strengthened joints (Alcocer and Jirsa, 1990). In an attempt to partially fill this gap, NIST, in an earlier phase of a multi-year research program on existing concrete buildings, carried out a joint study at Cornell University to design, construct, and test several joint strengthening techniques [Beres et al., 1992a, b, c].

- **The steel bracing technique** (See Phan, et. al. [1993, 1994] for references) involves attaching steel sections through the use of mechanical connectors to the existing LRC frames to supplement their lateral force resisting system. These steel sections are usually arranged into X-braces, K-braces, or V-braces. The steel braces can be concentrically or eccentrically added to existing LRC buildings. In concentrically braced frames, steel braces are inserted in the frame opening to enhance the ductility and strength of the existing concrete frame. In eccentrically braced frames, complete steel structural systems, which are continuous through the floor slabs and attached to the building exterior, can be designed to essentially replace the existing lateral force resisting system.

- **The column strengthening techniques** (See Phan, et. al. [1993, 1994] for references) involves either increasing the size of the column by enclosing the existing column with a new layer of concrete (either by CIP concrete or by pneumatically applied concrete) and additional reinforcement, or connecting external steel plates to the existing column. Most column strengthening techniques add transverse reinforcement in an attempt to improve ductility. These techniques are often generically termed "jacketing". Where the flexural capacity of the column is adequate, gaps are left at top and bottom of the jacketing to avoid increasing the flexural capacity and related induced shear forces.

Each of these techniques has both merits and technical or practical disadvantages. In general, the infill wall technique appears to result in the highest increase in lateral load capacity relative to other techniques, while the steel bracing technique appears to provide the greatest increase in ductility. However, despite the general knowledge obtained from experimental studies with regard to the effectiveness of each of these strengthening schemes, little guidance is available on how to assess quantitatively the increase in the toughness and ductility of existing lightly reinforced concrete (LRC) buildings due to the strengthening method.

This has resulted in the inability to assess *quantitatively* the effectiveness of a strengthening technique. Further, this limitation has precluded comparisons between potential schemes, so optimization of design has been nearly impossible. A recent publication by the Building Seismic Safety Council (BSSC) for the Federal Emergency Management Agency (FEMA), *NEHRP Handbook for Seismic Rehabilitation of Existing Buildings* [BSSC, 1992], identified many techniques for strengthening various types of existing buildings. This document

describes several strengthening schemes for LRC buildings and illustrates connections between the existing structure and the elements added for strengthening. While this document provides valuable insights into the practical aspects and the relative merits of the various retrofit techniques, still lacking is a method for the quantitative assessment of the improvement in seismic performance of a strengthened structure.

1.2 PROJECT OVERVIEW AND OBJECTIVES

In an effort to develop such quantitative assessment techniques and to complement other ongoing efforts by other federal agencies (Guidelines and Commentary for the Seismic Rehabilitation of Buildings, FEMA), a research study was initiated at the National Institute of Standards and Technology (NIST) with the overall aim of developing guidelines for seismic strengthening of LRC frame buildings. The technical approach in this multi-year research program is to utilize existing experimental research results to develop analytical techniques for evaluating quantitatively the effectiveness of common strengthening schemes. Guidelines for the seismic strengthening of LRC frame buildings will be developed based on the results of analytical evaluation.

To achieve the objective, a comprehensive literature survey of studies on strengthening methods was conducted [Phan et. al., 1993, 1994] at NIST. This literature search yielded numerous studies on seismic strengthening of LRC frames using various techniques with the most common listed in Section 1.1. From the available experimental data, the majority of the studies involved the use of infill wall technique, with only a limited number of tests on other techniques. For this reason, it was decided that the focus of this study would be to develop recommended design guidelines for the strengthening technique involving the use of infill walls.

Subsequently, experimental results from 54 tests of LRC frames were selected for this study. These tests results were subjected to a systematic examination, based on a statistical approach, where factors affecting the inelastic cyclic behavior of the LRC frames were considered as variables. The results are two sets of analytical equations: (1) the first set [Phan et. al., 1993] includes empirical equations describing the general inelastic behavior of existing and strengthened LRC frames in terms of three hysteretic failure parameters α, β, and γ; and (2) the second set [Phan et. al., 1994] includes empirical formulas for computing ultimate shear strength, P_u, story drift ratio at ultimate load d_u/H_c, and ductility factor μ_u, of the strengthened LRC frames. The two analytical tools are intended to complement each other. The aim for developing the first set of empirical equations (hysteretic failure models) was to provide a comprehensive analytical tool for computing the inelastic, hysteretic response of LRC structures when subjected to cyclic lateral loads. This type of analysis provides the complete response history of the LRC frames at each stage of loading or deformation up to failure. However, because the hysteresis failure models were developed for use with a research program IDARC (Inelastic Damage Analysis of Reinforced Concrete Structures, [Park et. al., 1987]) which requires substantial computational capability, the hysteresis failure models lend themselves primarily to research uses. For this reason, the second set of empirical equations was developed

using the same experimental database to provide a simplified method for computing the critical parameters such as P_u, d_u/H_c, and μ_u, of the strengthened LRC frames.

To date, the hysteretic failure models developed in this study have been partially validated using results of past experiments [Phan et. al., 1993]. Further validation of the applicability of the models for use in multi-bay multi-story LRC frames has been conducted in the past year and will be reported in this paper. Further, parametric study using the hysteretic failure models to examine the sensitivity of various design factors to the performance of strengthened LRC structures has been conducted. The results of the parametric study formed the basis for the design guidelines for seismic strengthening using the infill walls technique recommended in this report.

1.3 SCOPE OF THIS REPORT

Chapter 2 describes the validation of the hysteretic failure models for use in the analysis of multi-bay multi-story LRC frames.

Chapter 3 describes the parametric study conducted using these hysteresis parameters computed from the hysteretic failure models developed in this study. The parametric study include quasi-static and dynamic analyses of LRC frames subjected to a prescribed cyclic deformation history and to selected earthquake motions. Design parameters such as infill wall thickness, reinforcement ratios, and anchor area, were varied to study the effect of these design variables on the strengthened structures.

The results of the parametric study and observations from various experimental programs were used to form the basis for the recommended design guidelines for LRC frames described in Chapter 4.

2.0 VALIDATION OF HYSTERETIC FAILURE MODELS

2.1 GENERAL

The hysteretic failure models have been validated in the past [Phan et al., 1993] by using experimental results of a CIP infilled one-bay one-story frame specimen, tested by Aoyama [Aoyama et. al., 1984], and a one-bay three-story frame tested by Higashi [Higashi et. al., 1980, 1981]. The validation process included modeling of the test frames using the program IDARC, characterizing frame hysteretic behavior using the hysteretic failure models developed in this study [Phan, et. al, 1994], performing quasi-static dynamic analysis of the frames using the experimental deformation histories, and comparing analytical results with experimental results. For detailed discussions of these two validations, the readers are referred to previous publications of this study [Phan et al., 1993, 1994].

These two validations proved the applicability of the hysteretic failure models for the inelastic analysis of existing and strengthened LRC frames. However, those validations are for the cases of one-bay structures (one-bay, one-story and one-bay three-story) and since the hysteretic models were developed based on the results of one-bay, one-story experiments, questions still remain as to the validity of the hysteretic failure models for multi-bay structures. As multi-story, multi-bay construction is more common, it is necessary to validate the models' applicability for such cases. However, experimental data for multi-story multi-bay frames are extremely rare. In this study, a two-bay three-story LRC frame, tested by Yunfei et al. [Yunfei et. al., 1986], was modeled using the program IDARC and its hysteretic behavior was characterized by the hysteretic failure models to examine the applicability of these models in the case of multi-story, multi-bay construction. The description of the test frame and the analysis using IDARC are discussed in the following section.

2.2 ANALYSIS OF TWO-BAY THREE-STORY TEST FRAME

A pseudo dynamic test of a 1:2 scaled three-story two-bay LRC frame was conducted by Yunfei et. al. [Yunfei et. al., 1986]. The frame geometry and reinforcement details are shown in Figure 2.1. The test frame was subjected to 18 cycles of deformation, corresponding to 6 top-floor drift levels of 0.25%, 0.75%, 1.25%, 2.0%, 2.5%, and 3%. The experimental load-displacement history is shown in Figure 2.2. The loads and displacements given in Figure 2.2 correspond to the loads and displacements at the top of the floor.

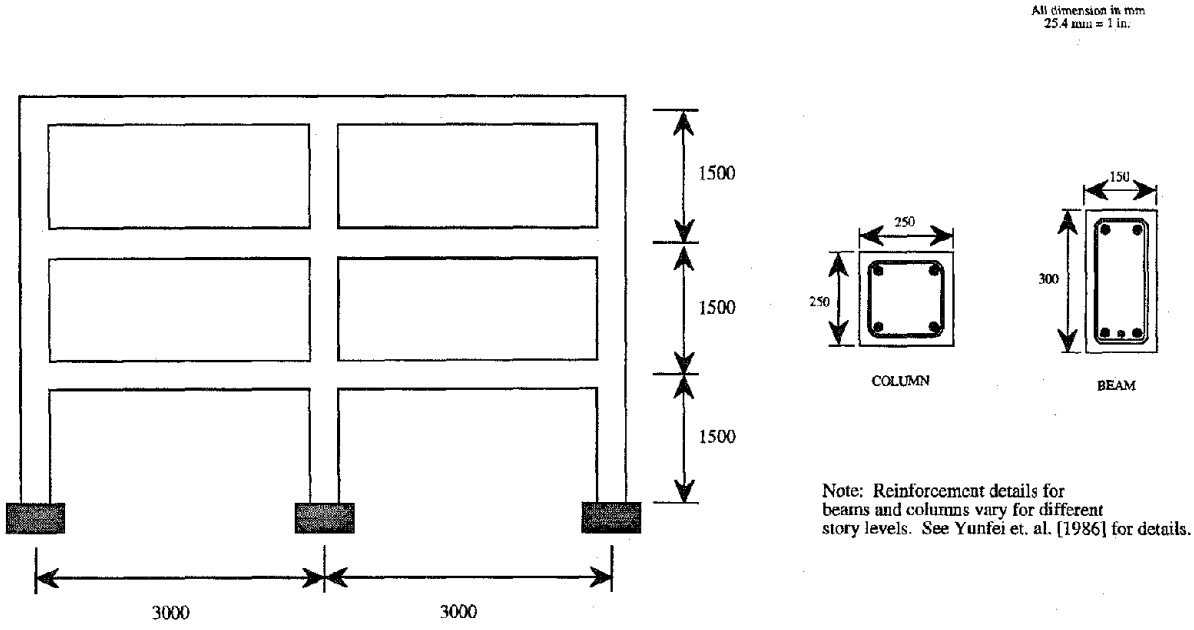

Figure 2.1. Yunfei's Frame.

The material properties that were used as input for the IDARC model were the same as that reported by Yunfei [Yunfei et. al., 1986] - a concrete compressive strength of 40.2 MPa (5.83 ksi) and a reinforcement yield strength of 400 MPa (58.01 ksi). The geometric and material properties of the frame were used in calculating the three hysteresis parameters α, β, γ in accordance with the equations for hysteretic parameters developed earlier [Phan et. al., 1993].

The IDARC model was created by replacing each bay of the frame with a set of corresponding hysteretic parameters α, β, γ. The model was then subjected to the same deformation history used in the experiment.

The result of the analysis, in the form of cyclic load-deformation response, is shown in Figure 2.3. Comparison of the analytical and experimental load-deformation histories shows an excellent match, in terms of structural stiffness and resulting shear forces, up to the third cycle of imposed drift at 1.25%. It should be noted that at this drift level, the frame has gone well into the inelastic range as can be observed from the experimental load-deformation history (Figure 2.2). Beyond a drift of 1.25%, the analytical model showed little strength degradation. In contrast, the experimental frame achieved a maximum shear capacity of 174 kN (39.1 k) at 1.25% and exhibited a gradual strength degradation thereafter.

The difference in shear capacity at higher drift levels between the experimental and the analytical model is probably due to the modeling technique used. In modeling the frame, each bay of the two-story, three-bay frame was assigned a set of hysteretic parameters α, β, γ, computed using the hysteresis models which were developed using the results of one-bay, one-story tests. Thus, for the adjacent bays which shared the same column, the shared column is accounted for twice when the hysteretic parameters were computed for each of the two bays. For this reason, the analytical model would be stronger than the actual test frame.

There is no simple, straightforward way to model the shared column at this stage since the hysteretic models were developed using one-bay, one-story experiments. However, it should be emphasized again that the model appears to be adequate in predicting the load-deformation behavior of the two-bay, three-story test frame up to a drift level that is well into the inelastic range (1.25%). At this drift level, extensive concrete cracking and yielding of the reinforcement have taken place. The analytical response is thus considered reasonably accurate and the models are deemed acceptable for use in predicting the hysteresis response of multi-story multi-bay LRC frames.

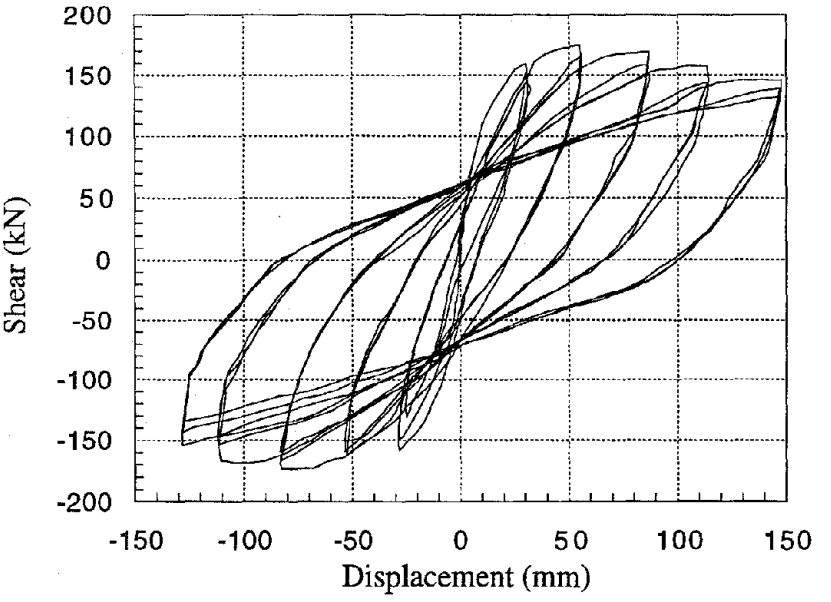

Figure 2.2. Experimental Load-Deformation History of Yunfei's Frame.

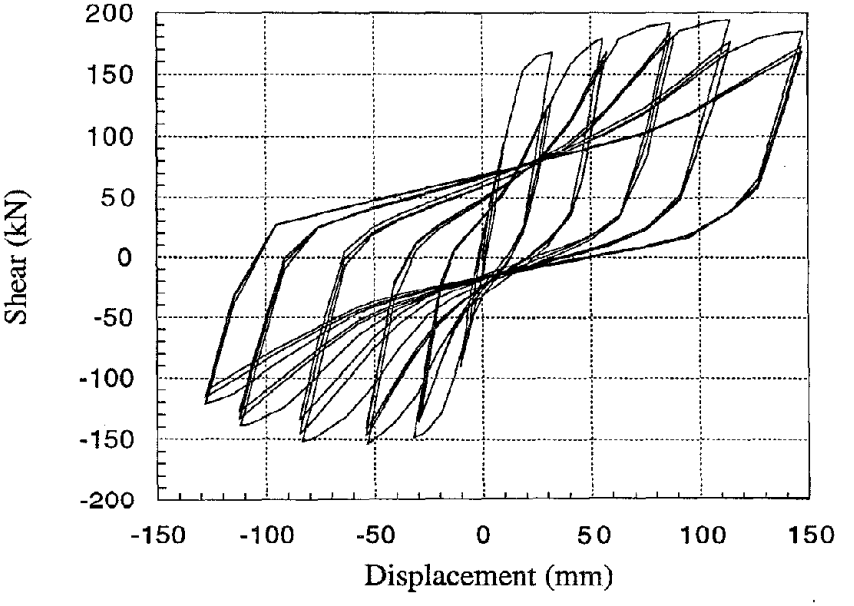

Figure 2.3. Analytical Load-Deformation History of Yunfei's Frame.

3.0 PARAMETRIC STUDY

3.1 INTRODUCTION

The empirical equations proposed in [Phan et al., 1993] to compute the three hysteretic failure parameters α, β, and γ, for LRC frames depend on many physical parameters or variables. These empirical equations were employed in a parametric study to assess the influence of different variables on the overall behavior of the LRC frames.

Specifically, the empirical equations were used to compute different sets of α, β, γ for a model LRC frame strengthened by two infill wall techniques: CIP infill wall and precast infill wall. Different combinations of α, β, and γ were obtained by varying such parameters as infill wall thickness, infill wall reinforcement ratio and the total cross sectional area of the anchors used in connecting the infill wall to the existing frame.

Relative differences in the overall hysteretic response of the frame, in terms of maximum shear capacity and story drift were used as the basis for design recommendations for the strengthening of LRC frames using the infill wall technique.

3.2 MODEL DESCRIPTION

A 1/2-scale model of a one-bay, one-story frame prototype frame was used in the parametric study. The frame was modeled using beam, column and wall elements. The moment-curvature envelopes for these elements were specified using three points: cracking, yield, and ultimate. For each model, one set of hysterectic failure parameters was computed to describe the hysteretic behavior of the frame. These parameters defined the behavior of the frame as a unit and not the behavior of individual elements. A sample input file for the program IDARC is given in Appendix A.

The dimensions of the beams were 150 mm (5.91 in.) by 300 mm (11.81 in.). The clear span of the beam was 2750 mm (108.27 in.). The clear height of the column was 1350 mm (53.15 in.) and the dimensions of the columns were 250 mm (9.84 in.) by 250 mm (9.84 in.). The length of the shear wall was 2750 mm (108.27 in.) and the thickness of the wall was varied. A different set of moment-curvature values were calculated for each wall thickness. The concrete compressive strength was 40.2 MPa (5.83 ksi) and the yield strength of the steel used was 400 MPa (58.01 ksi). The frame configuration and dimensions are as shown in Figure 3.1.

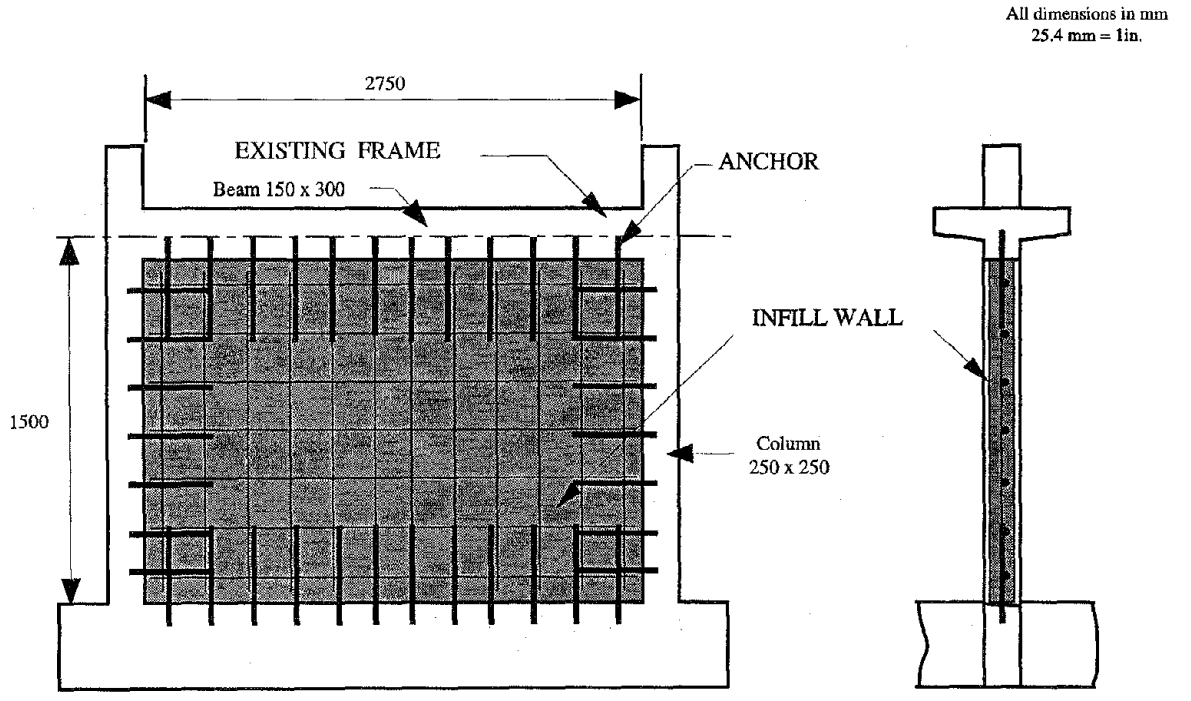

Figure 3.1. Configuration and Dimensions Frame used in Parametric Study.

3.3 DESCRIPTIONS OF VARIABLES

As mentioned in section 3.1, the effects on the overall behavior of the LRC frames of three variables were investigated. These three variables are considered to have the most significant influence on the overall behavior of LRC frames based on experimental observations. They include the thickness of the infill wall (t_w), the amount of wall reinforcement (ρ_w), and the cross sectional area of connecting anchors (A_c). These variables were examined for both CIP and precast infill wall techniques.

To study the influence of the infill wall thickness, the three hysteretic parameters α, β, γ corresponding to wall thicknesses ranging from 0 mm (existing frame) to 250 mm [0, 75 (2.94 in.), 100 (3.94 in.), 125 (4.92 in.), 150 (5.91 in.), 175 (6.89 in.), 200 (7.87 in.), 225 (8.86 in.), 250 mm (9.84 in.)] were computed. The maximum infill wall thickness was set to not exceed the column width [250 mm (9.84 in.)]. The length of the infill wall was equal to the clear span of the beam [2750 mm (108.27 in.)]. The reinforcement ratio in these frames were fixed at 0.5% and the anchor area was fixed at 600 mm^2 (0.93 in.^{2}). The variable infill wall thickness was examined for frames with CIP infill walls only. The case of no infill wall (t_w = 0 mm), was included for comparison purposes.

To study the influence of infill wall reinforcement ratio, ρ_w ($\rho_{vw} = \rho_{hw} = \rho_w$, where ρ_{vw} is the reinforcement ratio in the vertical direction of the infill wall, and ρ_{hw} is the reinforcement ratio in the horizontal direction of the infill wall) was varied from 0.1% to 1.2% in 0.1% increments. These ratios were varied between 0.3% to 0.9% in increments of 0.2% for the precast infill walls. These minimum and maximum ratios were set based on the upper and lower bounds used in the experiments that served as the basis for this study. The infill wall thickness for these frames was fixed at 125 mm (4.92 in.) and the connecting anchor area was set at 600 mm^2 (0.93 in^2).

The influence of the anchor area was studied by varying the anchor area from 5 cm^2 (0.78 in^2) to 15 cm^2 (2.33 in^2) in increments of 2.5 cm^2 (0.39 in^2) for frames with CIP infill walls and from 5 cm^2 (0.78 in^2) to 12.5 cm^2 (1.94 in^2) for frames with precast infill walls. The infill wall thickness was set at 125 mm (4.92 in.) and the infill wall reinforcement ratio was set at 0.5%. The embedment depth of the anchors was 125 mm (4.92 in.).

The different variations of the three variables are shown in Tables 3.1 to 3.5. Also, given in the tables are the corresponding three hysteresis parameters α, β, and γ.

Table 3.1. CIP Infill Walls, Vary Wall Thickness, t_w.

t_w [mm (in.)]	α	β	γ
0	39.12	0.95	0.10
75 (2.95)	31.86	0.83	0.27
100 (3.94)	28.21	0.77	0.36
125 (4.92)	24.54	0.70	0.45
150 (5.91)	20.82	0.64	0.54
175 (6.89)	17.12	0.58	0.63
200 (7.87)	13.34	0.52	0.71
225 (8.86)	9.54	0.45	0.80
250 (9.84)	5.70	0.39	0.89

Table 3.2. CIP Infill Walls, Vary Reinforcement Ratio, ρ_w.

ρ_w (%)	α	β	γ
0.1	33.94	0.66	0.35
0.2	31.59	0.67	0.35
0.3	29.24	0.68	0.35
0.4	26.89	0.69	0.35
0.5	24.54	0.70	0.35
0.6	22.18	0.71	0.35
0.7	19.83	0.73	0.35
0.8	17.48	0.74	0.35
0.9	15.13	0.75	0.35
1.0	12.78	0.76	0.35
1.1	10.43	0.77	0.35
1.2	8.08	0.78	0.35

Table 3.3. CIP Infill Walls, Vary Anchor Area, A_c.

A_c (cm^2) [A_c/A_w (%)]	α	β	γ
5.0 [0.30%]	28.42	1.47	0.71
7.5 [0.45]	21.11	1.32	0.51
10.5 [0.60]	13.80	1.18	0.31
12.5 [0.75]	6.49	1.04	0.11
15.0 [0.90]	0.64	0.92	0.01

Table 3.4. Precast Infill Walls, Vary Reinforcement Ratio, ρ_w.

ρ (%)	α	β	γ
0.30	13.84	1.04	0.77
0.50	12.48	1.23	0.77
0.70	11.11	1.43	0.77
0.90	9.75	1.63	0.77

Table 3.5. Precast Infill Walls, Vary Anchor Area, A_c.

A_c (cm_2) [$A_c/A_{w\ (\%)}$]	α	β	γ
5.0 [0.30%]	12.48	1.23	0.77
7.5 [0.45]	7.43	1.20	0.77
10.0 [0.60]	2.38	1.16	0.77
12.5 [0.75]	1.0	1.13	0.77

3.4 TYPE OF ANALYSIS

Two types of analysis, differentiated by the type of input motion, were used in the study. The first type of analysis involved input motion that was a prescribed displacement history for a quasi-static cyclic lateral load analysis. Results from these quasi-static analyses give an indication of the relative differences in the behavior of the frames in terms of the maximum shear force and maximum story drift experienced by the frames. These analyses also allow for the quantification of failure in terms of story drift. Failure was defined as the point at which the models achieved maximum shear force. This definition is chosen because the hysteretic failure model can accurately predict the maximum shear capacity but not so thereafter.

The prescribed displacement history was selected based on a series of story drifts (ratios of the relative displacement of a story to the story height). The selected drift levels in the prescribed displacement history, in percent, are as follows: 0.2, 0.25, 0.35, 0.5, 0.75, 1.0, 1.5, 2.0, 2.5, 3.0, 3.5, 4.0, 6.0, 8.0, 10.0, 12.0. The frames were subjected to 3 cycles at each story drift level. This prescribed displacement history is similar to those used in other test programs [Priestley, 1992]. For the bare frame (t_w = 0 mm), the prescribed displacement history included additional story drifts of 14%, 16%, and 18% in anticipation of higher ductility capacity. Figure 3.2 shows the displacement history used in the analyses.

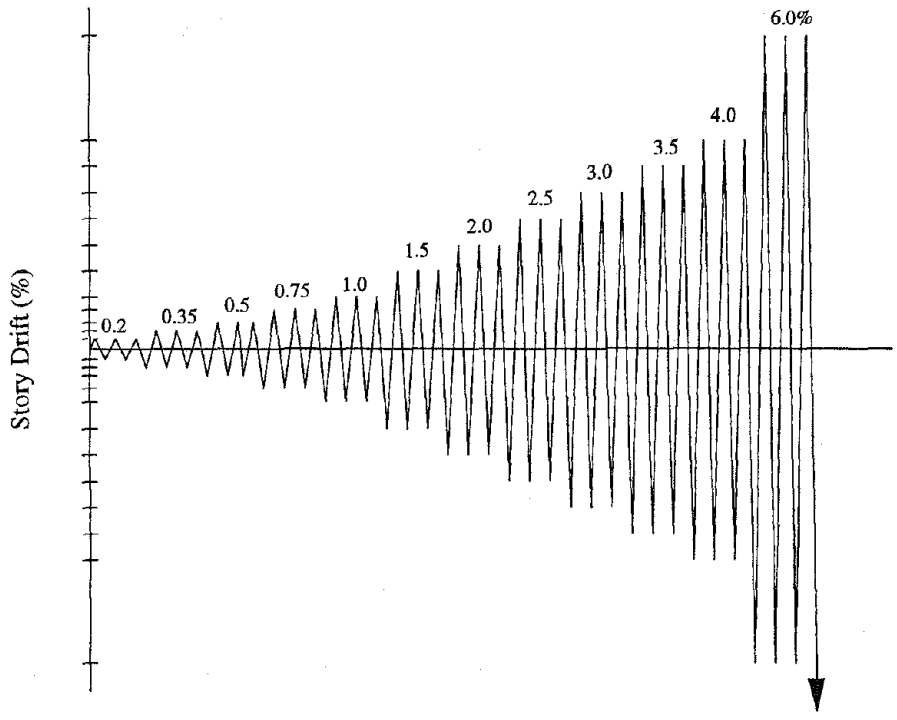

Figure 3.2. Portion of Prescribed Displacement History.

The second type of analysis involved input motion comprising actual acceleration records obtained from various earthquakes for transient dynamic analyses. The transient dynamic analyses were performed to examine the response of the LRC frames to random excitation and to include the effects of different soil types in the analyses. The selection of records were made from four past earthquakes: the 1971 San Fernando, 1979 Imperial Valley, 1987 Whittier, and 1989 Loma Prieta earthquakes. The selection of records was further narrowed by choosing free-field records only. For all the analyses, only the horizontal component of the record was used in the analysis and a 2% damping coefficient was used.

Spectral accelerations were calculated for the selected records and these were then compared with the UBC [ICBO, 1991] spectral acceleration curves for soil types S1, S2, and S3. The amplitudes of the accelerations were then multiplied by a scale factor chosen so that the sum of the differences (error) between the scaled accelerations and the values from the UBC curve were minimized for periods between 0.1 s to 0.5 s. This period range was selected because the expected periods of the prototype frames would likely fall within this range [Period, T, $\approx$ 0.1 x No. of Stories]. For each soil type, four acceleration records were chosen. This final selection was based on records with the smallest error and a scale factor that was close to 1.0. The selected acceleration records are shown in Table 3.6.

Table 3.6. Acceleration Records Used for Dynamic Analysis.

Eq. No.[a]	Record Name (Component)	Earthquake	Soil Type	Scale Factor
1	Corralitos (90)	Loma Prieta	S1	1.081
2	Gilroy 1 (360)	Loma Prieta	S1	0.988
3	Santa Cruz (90)	Loma Prieta	S1	1.044
4	Superstition Mt. (135)	Imperial Valley	S1	1.948
5	8224 Orion Blvd. (0)	San Fernando	S2	1.656
6	Cal. Tech. JPL (98)	San Fernando	S2	1.935
7	Hollywood Storage (90)	San Fernando	S2	2.592
8	Pump. Plant, Pearblossom (270)	San Fernando	S2	3.451
9	El Centro, Diff. Array 3 (180)	Imperial Valley	S3	1.061
10	Dogwood Rd, El Centro, Array 1 (180)	Imperial Valley	S3	0.946
11	Gilroy 2 (90)	Loma Prieta	S3	1.208
12	James Rd, El Centro Array 5 (230)	Imperial Valley	S3	0.896

[a] The earthquakes in the report will be referred to by these numbers.

The acceleration record for Earthquake 4 (Superstition Mountain), is shown in Fig. 3.3a and the spectral acceleration in Fig. 3.3b. Superimposed on Fig. 3.3b is the UBC response spectrum for soil type 1.

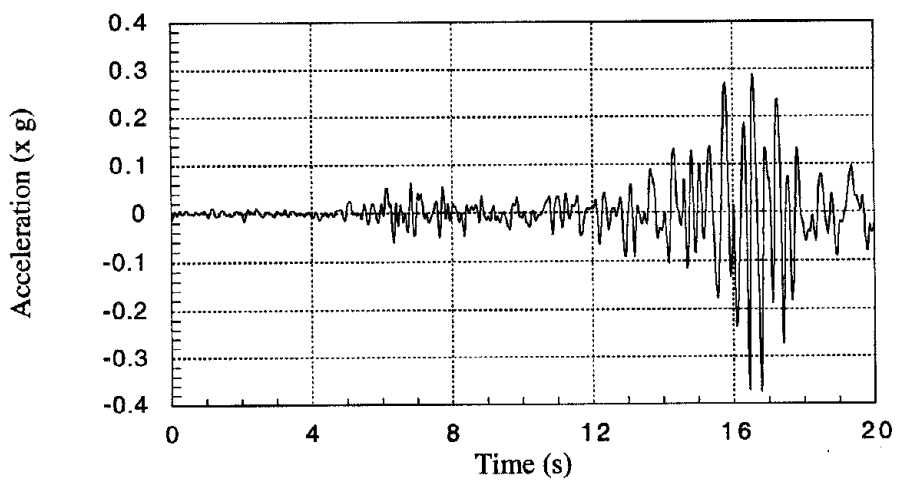

Figure 3.3a. Acceleration Record for Earthquake 4 Superstition Mountain, Imperial Valley.

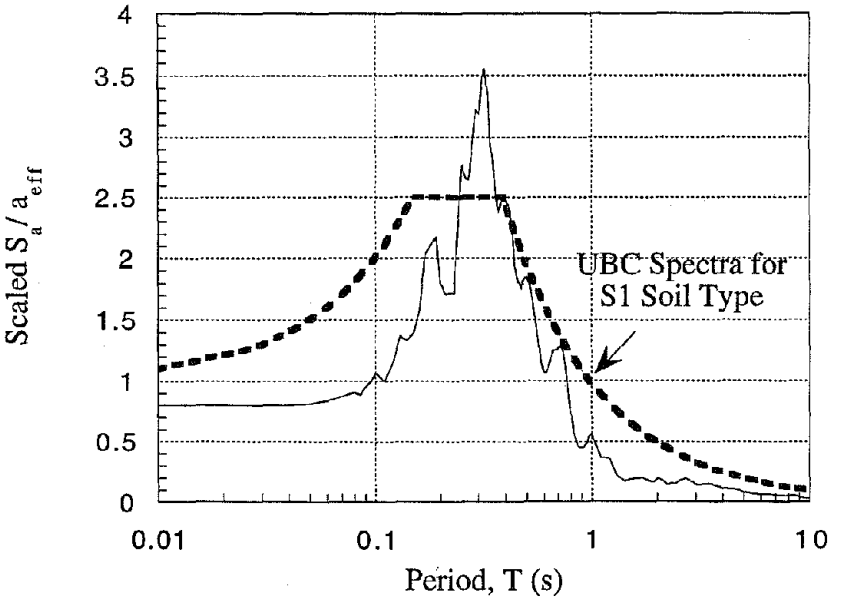

Figure 3.3b. Spectral Acceleration for Earthquake 4.

Initial analyses were made using the acceleration records scaled by the factors given in the last column in Table 3.6. The results indicated that the models remained in the elastic range and experienced very small story drifts. The models remained elastic because they were short, squat structures. Therefore, after several trial runs using various values of maximum horizontal acceleration, a maximum horizontal acceleration of 3g was chosen for all the dynamic analyses. Results from these analyses indicated that the models went into the inelastic range and achieved story drifts that ranged from 2% - 10%, in general. The reason for wanting this range of drifts was that the quasi-static analyses indicated a minimum of 3% story drift was achieved by these models at failure.

3.5 RESULTS OF PARAMETRIC STUDY

The maximum story drift is defined, hereinafter, as the story drift that corresponds to the maximum shear force obtained. Thus, based on the failure criteria defined in Section 3.4, the maximum story drift and the maximum shear force are the story drift capacity and the shear capacity. Desirable frame behavior is an increase in the drift capacity, the shear capacity, or both. The choice between increased drift or shear capacity would be based on analyses to determine the requisite demand of both.

It should be made clear that the drift capacities obtained from the analyses in this report are capacities of one bay, one story frame models. The capacity of a structure is likely to be much less than the capacities sited for the models or "components".

3.5.1 QUASI-STATIC ANALYSIS

3.5.1.1 CIP Infill Wall, Vary t_w

The maximum story drifts and maximum shear forces obtained for different values of wall thicknesses are shown in Figures 3.4 and 3.5, respectively. The maximum story drifts achieved by the bare frame model was 12%. The maximum story drifts of frames with infill walls decrease with increasing wall thicknesses. The rate of decrease of the maximum story drift is reduced for values of t_w= 150 mm (5.91 in., 3/5 of column width) and higher. For t_w = 75 mm (2.95 in.) to 250 mm (9.84 in.), the maximum story drifts varied from 8% [t_w = 75 mm (2.95 in.)] to a minimum of 4% [t_w = 250 mm (3.84 in.)]. The maximum story drifts remained at 4% for wall thicknesses of 150 mm (5.91 in.) to 250 mm (9.84 in.).

As expected, the maximum shear force of the frames increased with increasing wall thickness with the higher rate of shear capacity increase occurring at a value of t_w= 100 mm (3.94 in., 2/5 of column width). The maximum shear force ranged from approximately 170 kN (38.2 k, for t_w = 0 mm) to 450 kN [101.2 k, for t_w = 250 mm (9.84 in.)]. When compared to the frame without an infill wall, the shear force increased by a factor of approximately 2.5 for the frame with an infill wall thickness of 250 mm (9.84 in.).

The energy dissipated per cycle increased as the wall thickness increased. There is no clear relationship between the cumulative energy dissipated to failure and wall thickness as shown in Figure 3.6. The cumulative energy dissipated is defined as the summation of the cyclic energy dissipated to failure. The drop in the cumulative energy dissipated for the model with the 150 mm (5.91 in.) infill is a result of the lower story drift capacity obtained by that model.

The results shown in Figures 3.4 and 3.5 indicate that for a CIP infill wall, higher shear capacities can be achieved with little or no reduction in the story drift capacity for cases in

which the wall thickness is at least 2/5 the thickness of the adjacent columns. This is consistent with observations made from many of the experimental programs.

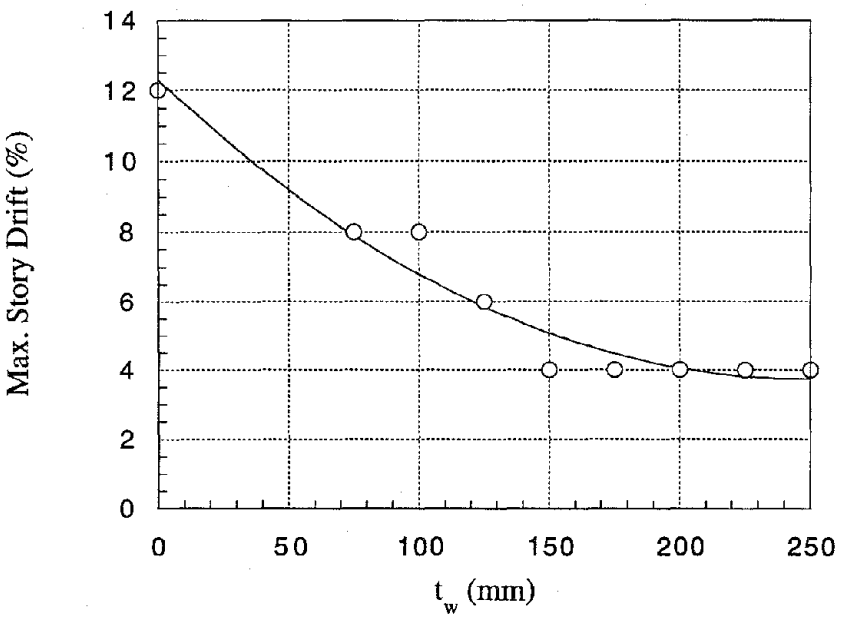

Figure 3.4. Maximum Story Drift for CIP Infill Walls, Vary t_w.

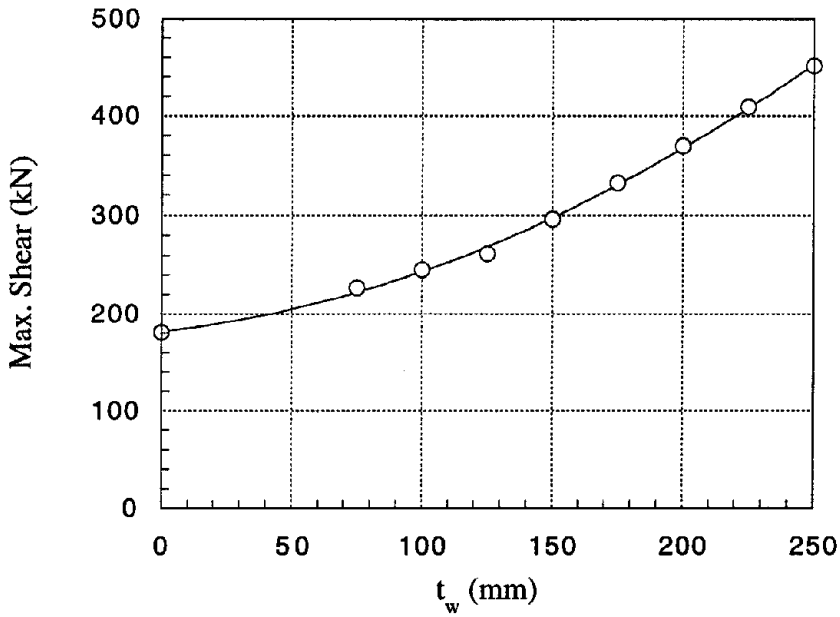

Figure 3.5. Maximum Shear for CIP Infill Walls, Vary t_w.

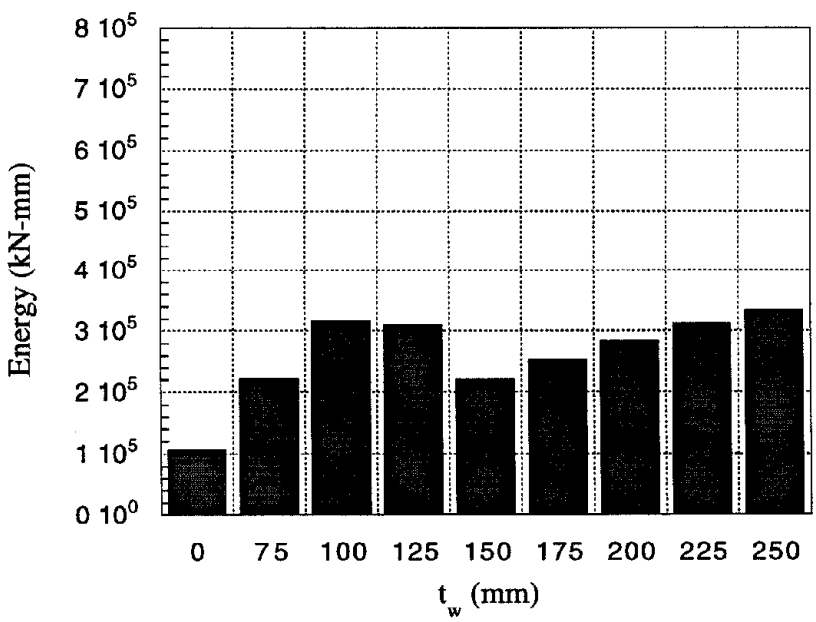

Figure 3.6. Cumulative Energy Dissipated, Vary t_w.

3.5.1.2 CIP Infill Wall, Vary ρ_w

The maximum story drift, maximum shear, and the cyclic energy dissipated corresponding to different values of infill wall reinforcement ratios ρ_w are shown in Figures 3.7 to 3.9, respectively. Figures 3.7 to 3.9 show a maximum value of 8% story drift was obtained for all models for ρ_w values of 0.1% to 1.2%. The maximum shear force obtained for all models was approximately 290 kN (65.2 k). The cumulative energy dissipated to failure decreased very slightly as ρ_w increased.

Neither the maximum story drift, the shear strength, nor the dissipated energy seem to be affected by increasing the infill wall reinforcement ratios. There are no clear experimental data to verify this observation since infill wall reinforcement ratio was not a variable in any of the experimental programs reviewed. Comparison between different experimental programs to isolate the effect of infill wall reinforcement ratios is rather difficult due to the influence of other variables such as specimen sizes, loading histories, material properties, etc. However, the analyses showed that although the infill wall yielded in flexure, the frames continued to carry additional lateral load until the beam yielded at both ends. After obtaining this peak value, the lateral load dropped off in the subsequent cycles. Therefore, if the wall did not fail in shear and the failure was caused by the failure of the frame, the additional reinforcement in the walls would not have affected the performance of the frame.

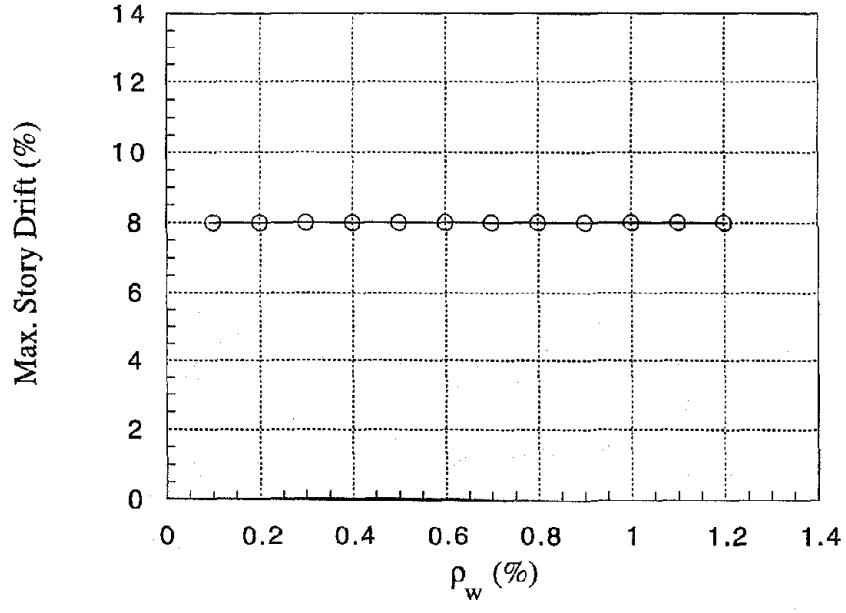

Figure 3.7. Maximum Story Drift for CIP Infill Walls, Vary ρ_w.

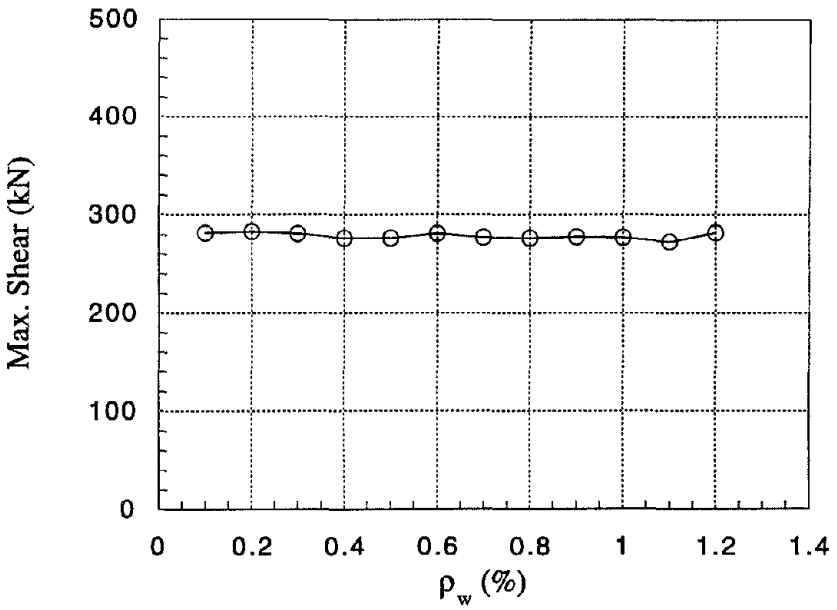

Figure 3.8. Maximum Shear for CIP Infill Walls, Vary ρ_w.

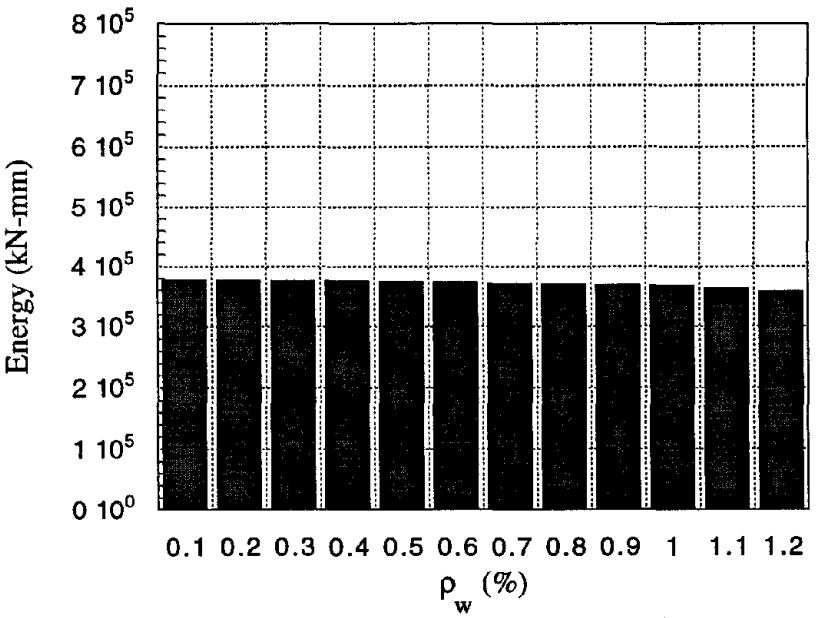

Figure 3.9. Cumulative Energy Dissipated to Failure.

3.5.1.3 CIP Infill Walls, Vary A_c

The maximum story drifts, maximum shear strength, cumulative dissipated energy, and hysteresis responses for different values of A_c are shown in Figures 3.10 to 3.14, respectively. For these analyses, the infill wall thickness was kept constant at 125 mm (4.92 in.), and an anchor embedment depth of 125 mm (4.92 in.) was used. This embedment depth was used in most of the experimental programs without any anchor pull-out problems. The anchor cross sectional areas were varied between 500 mm^2 (0.78 in^2) to 1500 mm^2 (2.33 in^2) in 250 mm^2 (0.39 in^2) increments. These corresponded with ratios of A_c/A_w of 0.3% to 0.9%, where A_w is the area of the infill wall at the wall/frame interface. It should be noted that the A_c/A_w ratios used in various experimental programs surveyed in [Phan et. al., 1993] ranged from 0.3% [Higashi et. al., 1980] to 0.81% [Aoyama et al., 1984 and 1986]. The lower value of A_c/A_w (0.3 to 0.4%) was reported to result in premature failure of the connection between the infill wall and the existing LRC frames. The analytical results show an increase in story drift for A_c greater than 750 mm^2 (1.16 in^2, A_c/A_w = 0.45%).

The maximum shear force appears to increase slightly as the anchor area is increased (Figure 3.11). The cumulative energy dissipated increases as the anchor area increased due to the higher story drifts achieved. However, the hysteresis curves for the model with A_c/A_w = 0.9% (Figure 3.14) are very narrow and exhibit a lot of pinching. As a result, the cyclic energy dissipated for the case of A_c/A_w = 0.9% is the lowest from among all cases. The hysteresis curves for the case with A_c/A_w = 0.75% is shown in Figure 3.13 for purposes of comparison. A comparison of the cumulative energy dissipated is given in Figure 3.12.

These analytical results indicate that the desirable A_c/A_w ratios for appreciable gain in maximum story drift and some gain in shear strength should be greater than 0.45%. As mentioned earlier, successful performance of the infill wall/existing frame system has been observed with A_c/A_w= 0.81%.

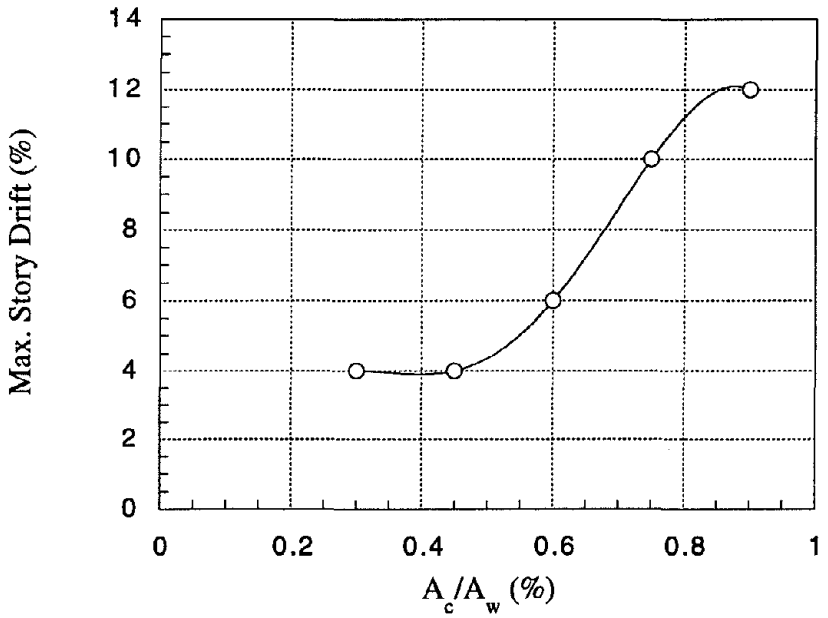

Figure 3.10. Maximum Story Drift for CIP Infill Walls, Vary A_c/A_w.

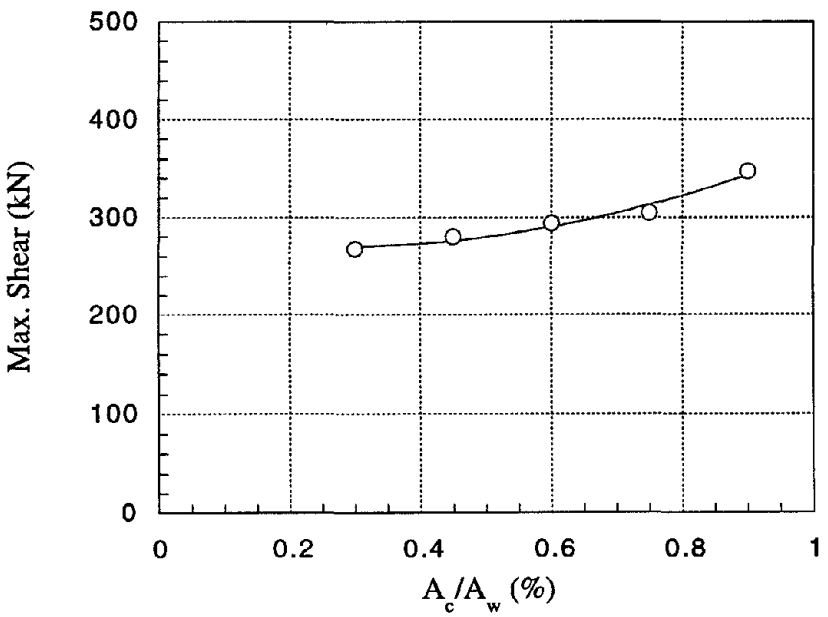

Figure 3.11. Maximum Shear for CIP Infill Walls, Vary A_c/A_w.

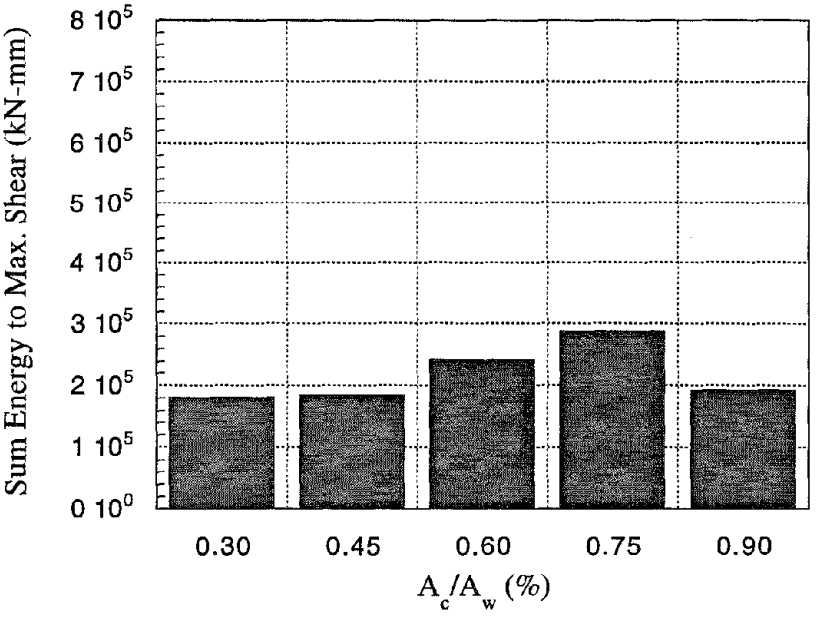

Figure 3.12. Cumulative Energy Dissipated to Failure.

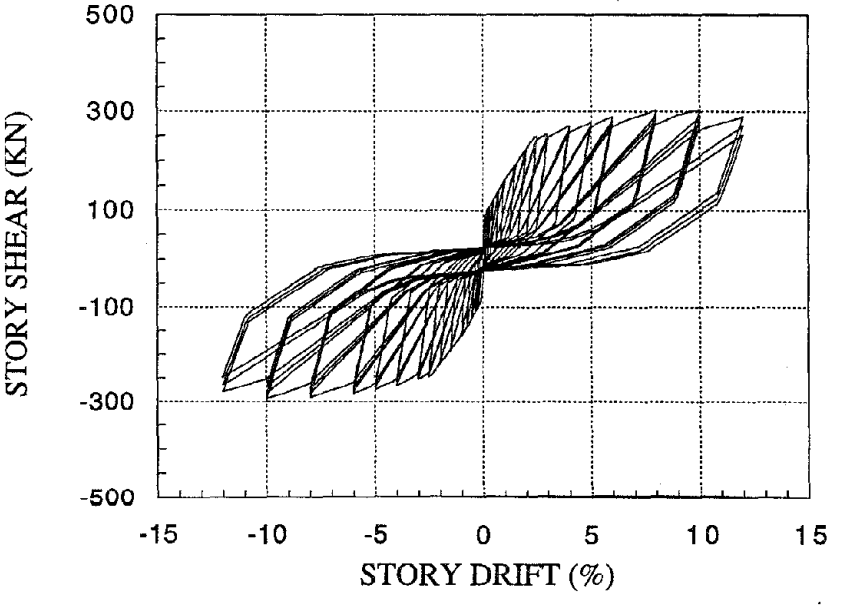

Figure 3.13. Hysteresis Curves, A_c/A_w=0.75%.

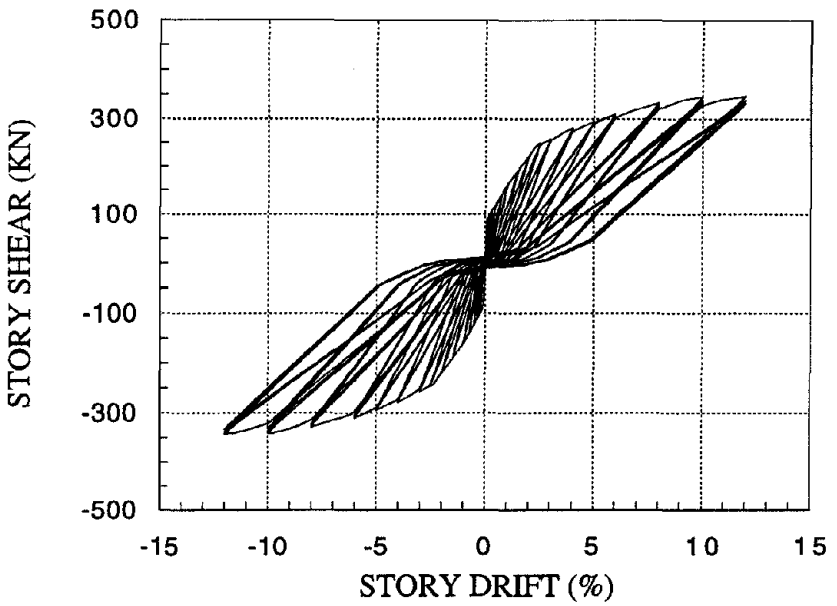

Figure 3.14. Hysteresis Curves, A_c/A_w=0.9%.

3.5.1.4 Precast Infill Walls, Vary ρ_w

For the precast infill wall technique, the infill wall consisted of three precast panels of the same height [1350 mm (53.1 in.)] and width [915 mm (36.0 in.)]. The thickness of the precast panels was fixed at 125 mm (4.92 in.). The reinforcement ratios of the precast panels were varied between 0.3% to 0.9%.

Similar to the case of CIP infill wall technique, the influence of reinforcement ratios of the precast panel on the maximum story drift and shear strength of the strengthened frames appeared to be negligible. The shear strength attained for different values of ρ_w ranged from approximately 250 kN (56.2 k) to 290 kN (65.2 k). The cyclic energy dissipated does not appear to be influenced by increasing ρ_w. The increase in the cumulative energy dissipated for increased values of ρ_w is a result of the higher drift obtained for these models. Figures 3.15 to 3.17 show the maximum story drift, maximum shear, and cumulative energy dissipated, respectively.

From Fig. 3.15, the maximum drift capacity for ρ_w of 0.5% is 4%. This is compared to the maximum drift capacity of 6% for the CIP infill wall with t_w = 125 mm (4.92 in.). This seems to contradict one of the conclusions drawn from the experimental tests which indicated that the frame strengthened with precast infill walls is more ductile than one strengthened with CIP infill walls. Further refinement of the empirical equations for calculating the hysteretic

parameters may be needed to eliminate this discrepancy. The reader should keep in mind that these equations were derived based on 55 experimental tests which were all that were available at the time. Also, from among the 55 tests, there were 93 variables which could possibly have an effect the computation of the hysteretic parameters. In addition, variables such as different loading history and scale factor cannot easily be quantified.

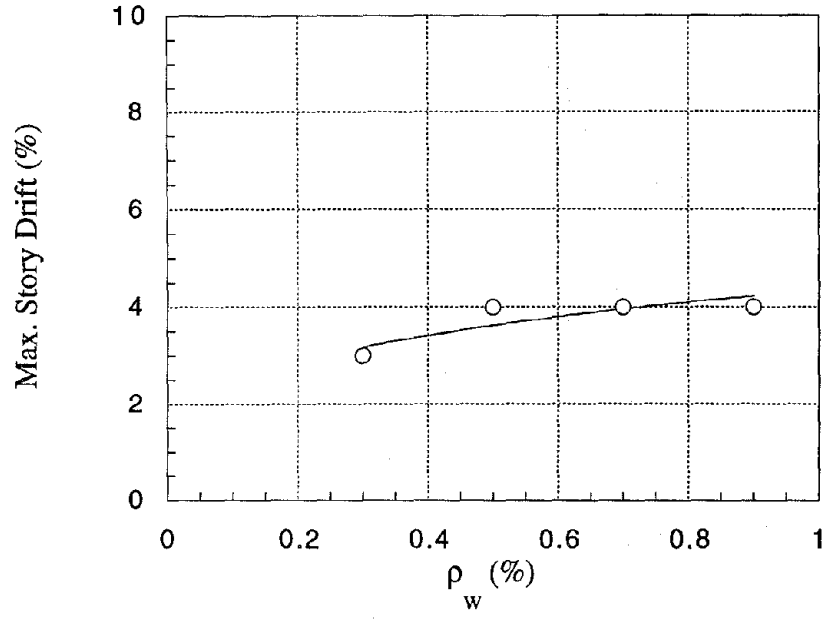

Figure 3.15. Maximum Story Drift for Precast Infill Walls, Vary ρ_w.

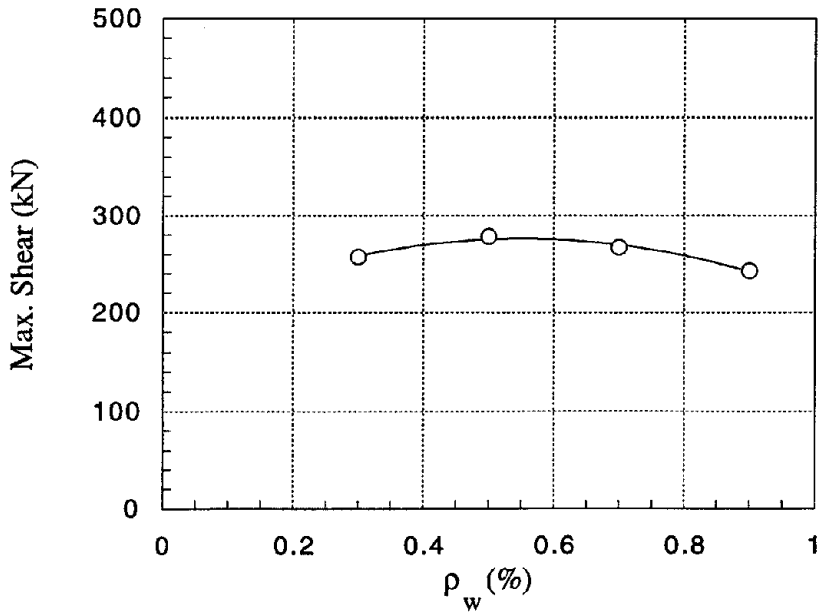

Figure 3.16. Maximum Shear for Precast Infill Walls, Vary ρ_w.

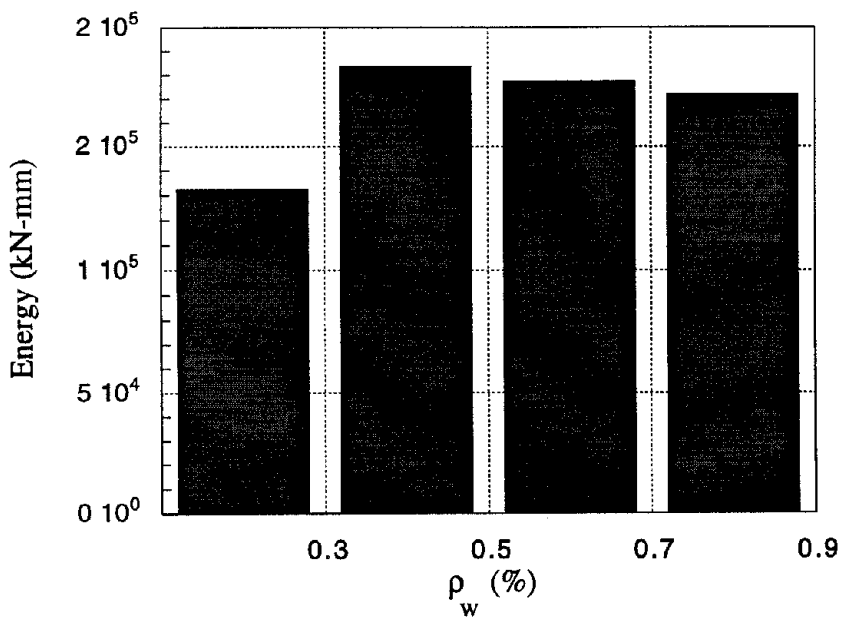

Figure 3.17. Cumulative Energy Dissipated.

3.5.1.5 Precast Infill Walls, Vary A_c

To study the influence of the anchor cross sectional areas on LRC frames strengthened by precast infill panels, the anchor areas were varied between 500 mm^2 (0.78 in^2) to 1250 mm^2 (1.94 in^2, A_c/A_w = 0.3% to 0.75%). The plots of the maximum story drifts, maximum shears, and cumulative energy dissipated are shown in Figures 3.18 to 3.20, respectively. Both the story drift and shear strength increased with increasing anchor areas, with the increase in shear strength much less significant than the increase in maximum story drift, which is similar to the case of CIP infill wall. The increase in cumulative energy dissipated for higher anchor areas is due to the higher drift obtained by these models.

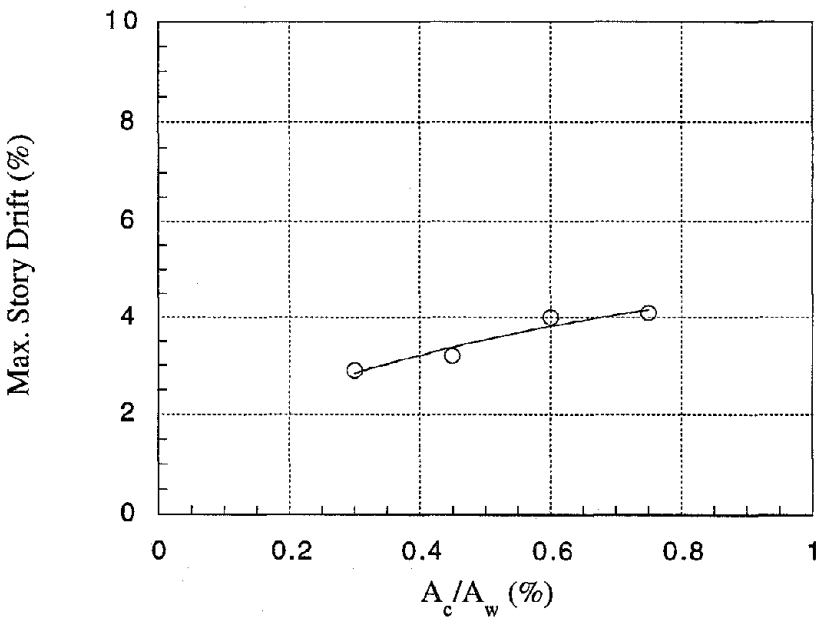

Figure 3.18. Maximum Story Drift for Precast Infill Walls, Vary A_c/A_w.

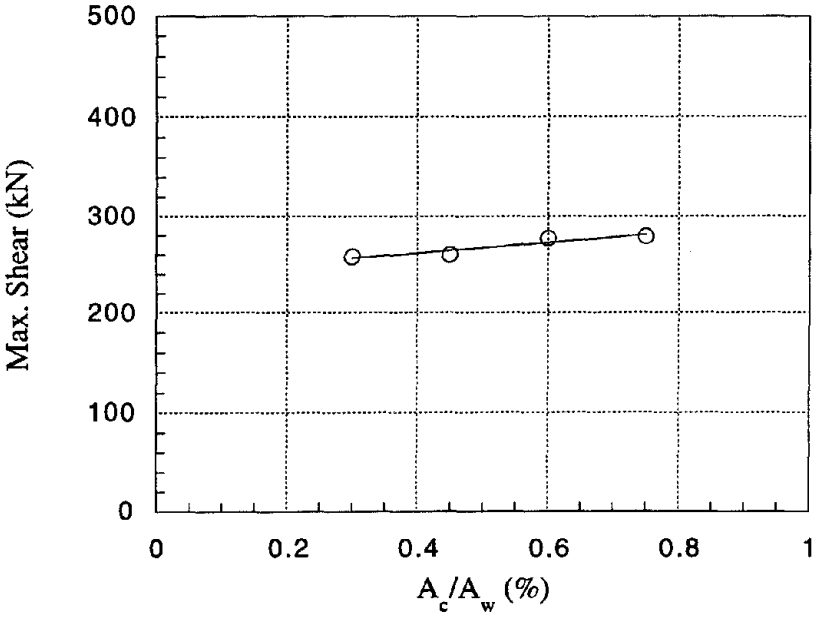

Figure 3.19. Maximum Shear Force for Precast Infill Walls, Vary A_c/A_w.

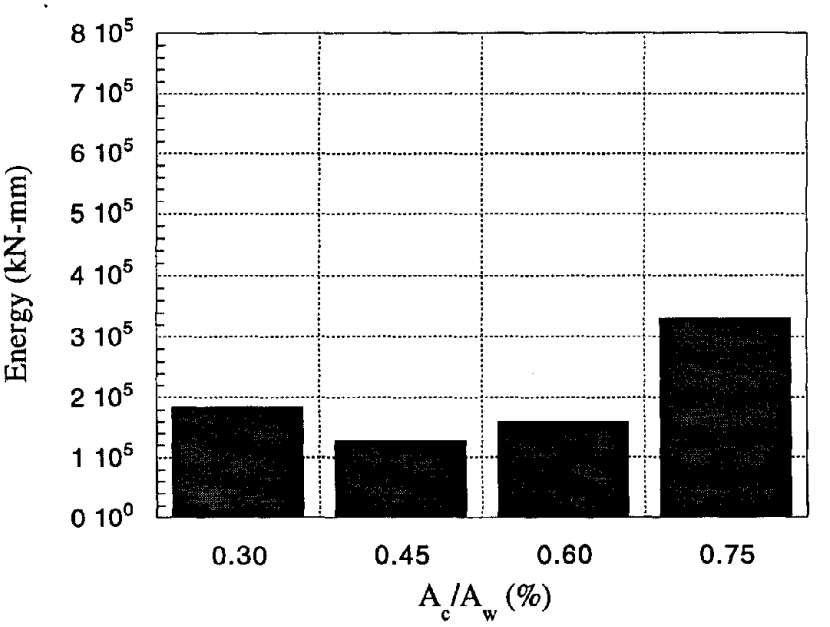

Figure 3.20. Cumulative Energy Dissipated.

3.5.2 DYNAMIC ANALYSIS

As mentioned in Section 3.4, dynamic analyses were performed to examine the responses of the LRC frames to random excitation and to examine the effect of different soil types. The spectral accelerations of acceleration records selected from past earthquakes are listed in Table 3.6. These were compared with the UBC [ICBO, 1991] curves for soil types S1, S2, and S3. For each soil type, four acceleration records were chosen as input motions for the dynamic analyses. The same one-story one-bay frames, infilled with CIP and precast panels, analyzed in the previous sections were used in the dynamic analyses.

3.5.2.1 CIP Infill Walls, Vary t_w

The infill wall thickness was varied between 0 mm to 250 mm (9.84 in.), similar to the quasi-static analysis. Due to the small aspect ratio (height to base length ratio) of the frame (one-bay, one-story frame), it was necessary to scale the maximum horizontal acceleration used in these analyses to 3g in order to force the strengthened frames into the inelastic and ultimately the failure ranges. Figures 3.21 to 3.23 show the trends for the maximum story drift by soil types (S1 to S3). The nomenclature, EQ. 1, EQ. 2, ... , EQ. 12, in the legend of these figures correspond to earthquakes 1 to 12 as listed in Table 3.6.

In general, for 75 mm (2.95 in.) $\leq t_w \leq$ 100 mm (3.94 in.), the maximum story drifts ranged from 3.5% to 11.5%. For $t_w \geq$ 100 mm (3.94 in.), the maximum story drifts ranged from 0.2% to 4% with the higher end drifts corresponding to the models with lower wall thicknesses. Based on these plots, a minimum wall thickness t_w of 100 mm (3.94 in., 2/5 of column width) limits the maximum story drift to 3% or less. A wall thickness of 200 mm (7.87 in., 4/5 of the column width) would limit the maximum story drifts of approximately 1% or less. No appreciable difference in the maximum story drifts was noted for the different soil types.

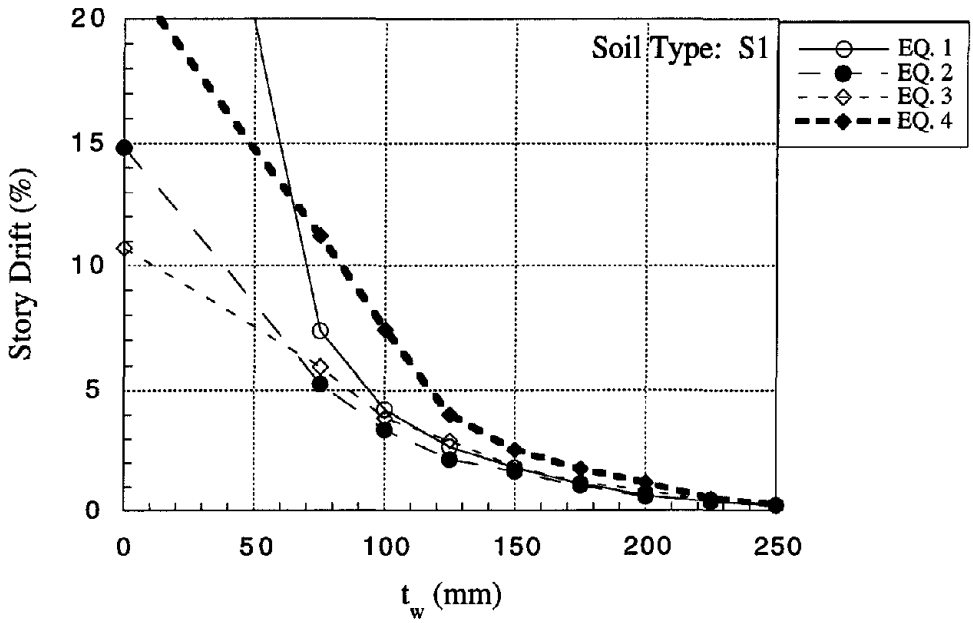

Figure 3.21. Maximum Story Drift, Vary t_w, Soil Type 1.

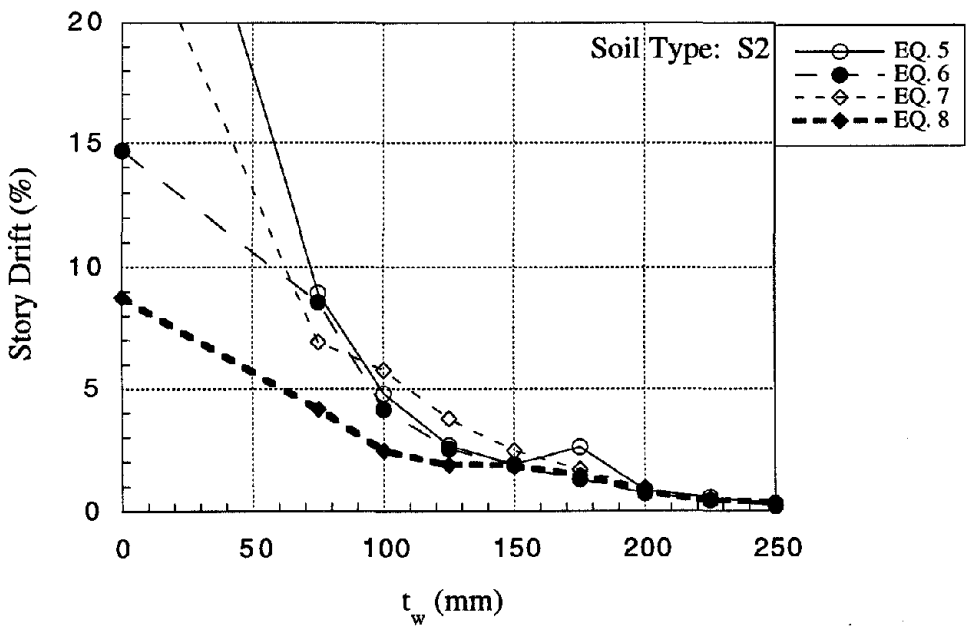

Figure 3.22. Maximum Story Drift, Vary t_w, Soil Type 2.

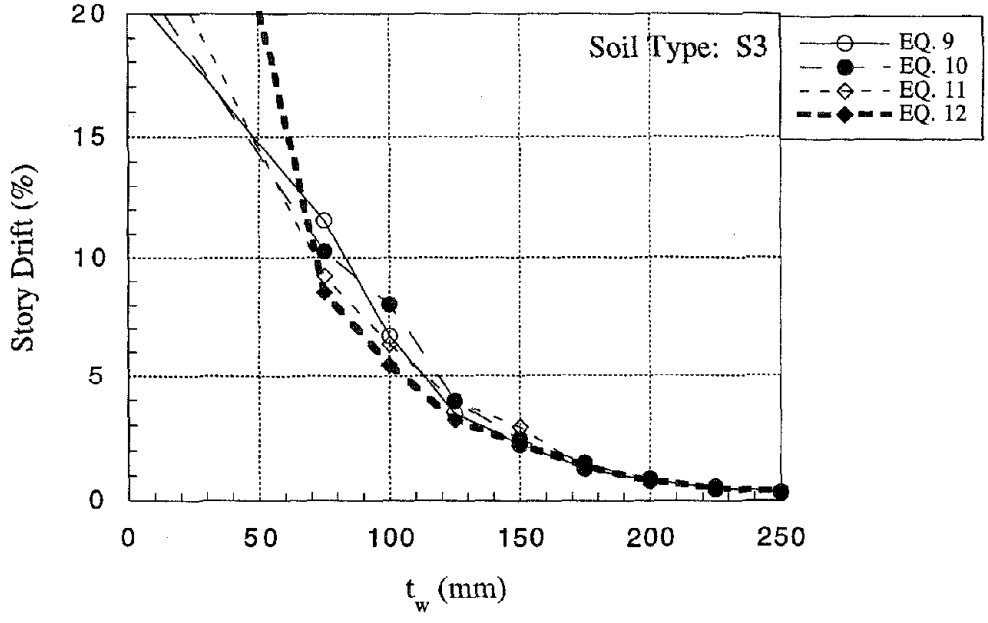

Figure 3.23. Maximum Story Drift, Vary t_w, Soil Type 3.

The maximum shear obtained remained approximately constant with increasing infill wall thickness for a given earthquake record, but a reduction in the shear force for t_w = 175 mm (6.89 in.) to 250 mm (9.84 in.) was observed for all input records (Figs. 3.24 to 3.26). This reduction in shear force is attributed to the fact that the period of the frame decreases as the wall thickness increases. Since the frame is only one story, the period of the frame is at the lower end of the response spectrum [T = 0.082 s for t_w = 50 mm (1.97 in.)]. Therefore, a further reduction in the period would correspond to lower forces to the structure. This is corroborated by the analyses which showed that the frames [$t_w \geq$ 175 mm (6.89 in.)] remained in the elastic range while the frames with $t_w <$ 175 mm (6.89 in.) sustained some damage. As with the story drifts, no appreciable difference was noted in the maximum shear force for the different soil types.

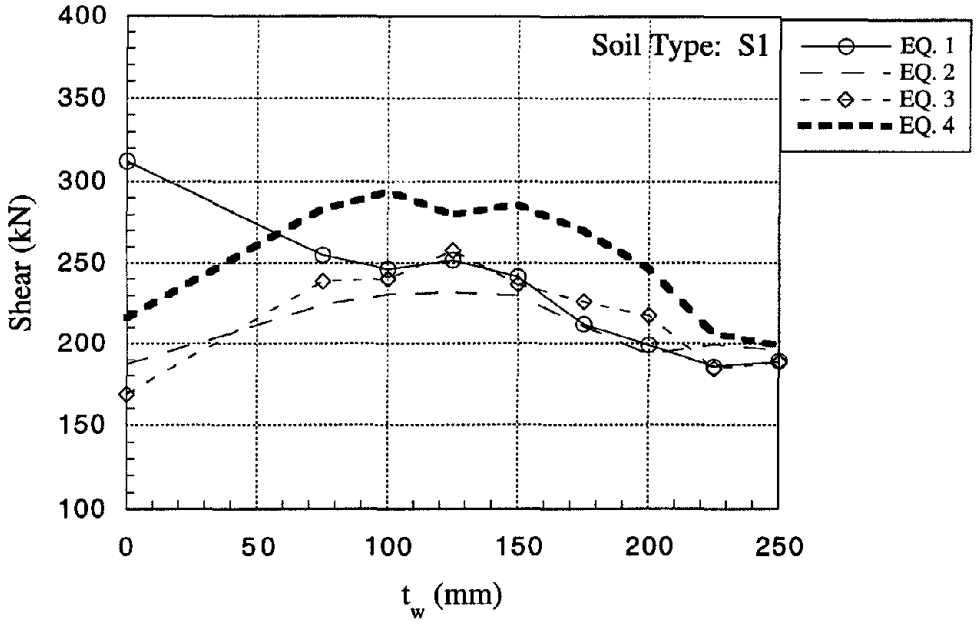

Figure 3.24. Maximum Shear Force, Vary t_w, Soil Type 1.

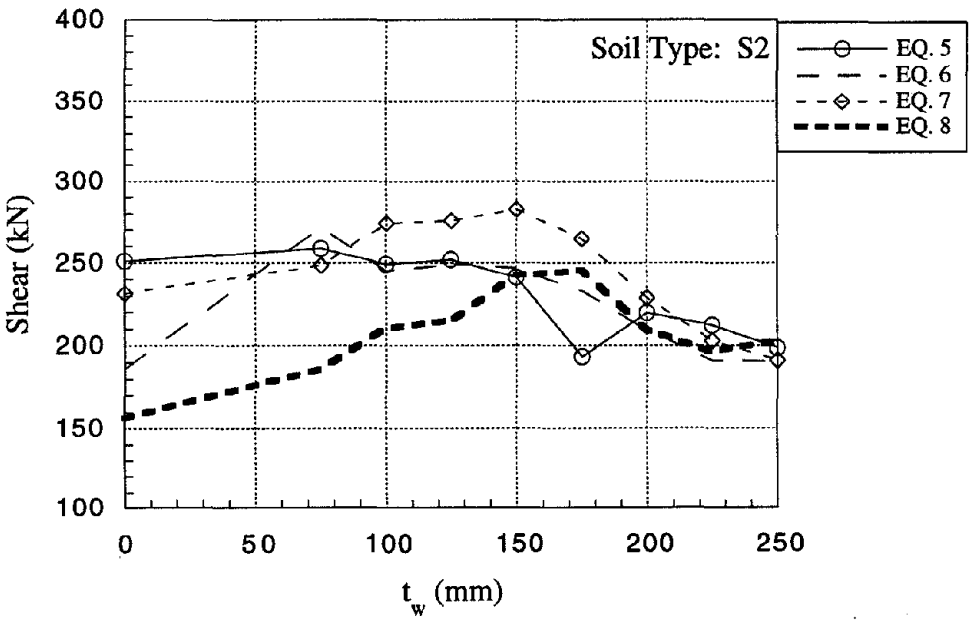

Figure 3.25. Maximum Shear Force, Vary t_w, Soil Type 2.

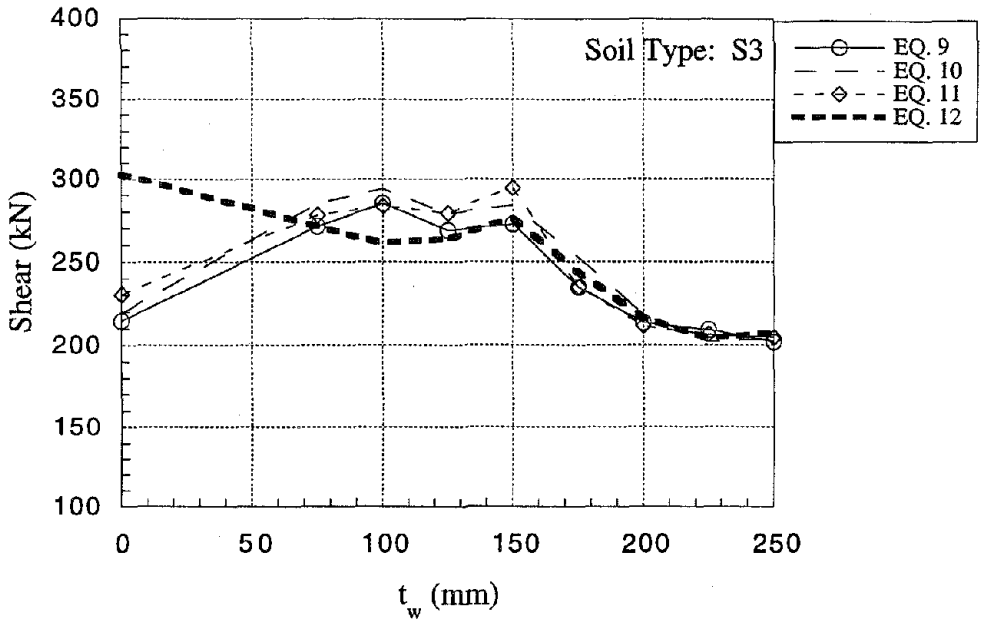

Figure 3.26. Maximum Shear Force, Vary t_w, Soil Type 3.

3.5.2.2 CIP Infill Walls, Vary ρ_w

For all soil types and earthquake records, there was insignificant variation in the maximum story drift and shear strength with increasing ρ_w values. From Figs. 3.27 and 3.28, it appears that the drift demand is more dependent on the input ground motion.

The maximum story drifts varied from 2% to 5% for soil types 1 and 2 and from 3.5% to 5% for soil type 3. This observation is similar to the case of quasi-static analysis. The maximum shear values ranged from approximately 220 kN (49.5 k) to 300 kN (67.4 k) with the values for soil type 3 being more tightly banded [268 kN (60.3 k) to 290 kN (65.2 k)]. The plots for the maximum drifts and shears are given in Figures 3.27 to 3.32.

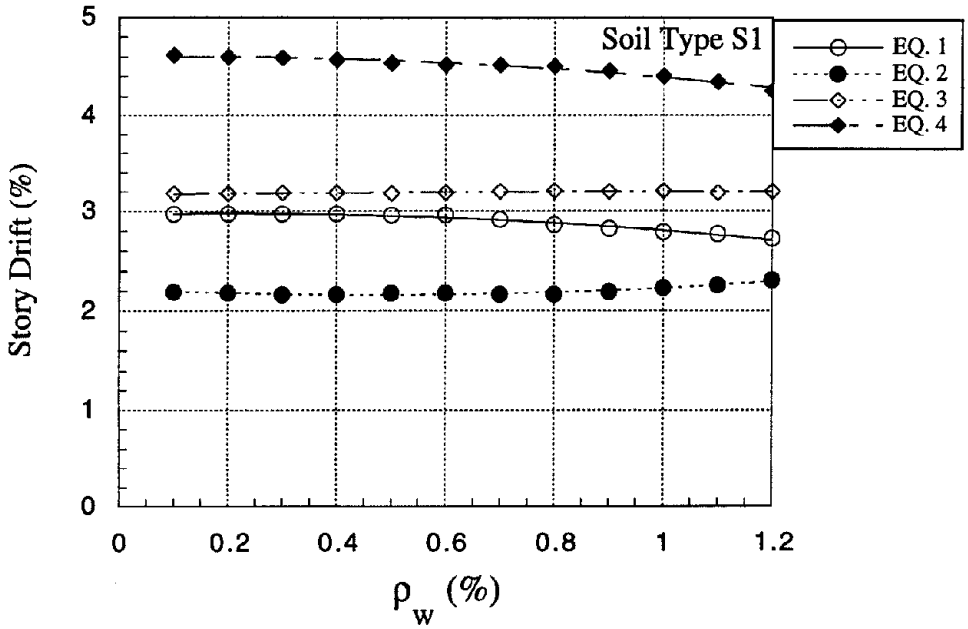

Figure 3.27. Maximum Story Drift, Vary ρ_w, Soil Type 1.

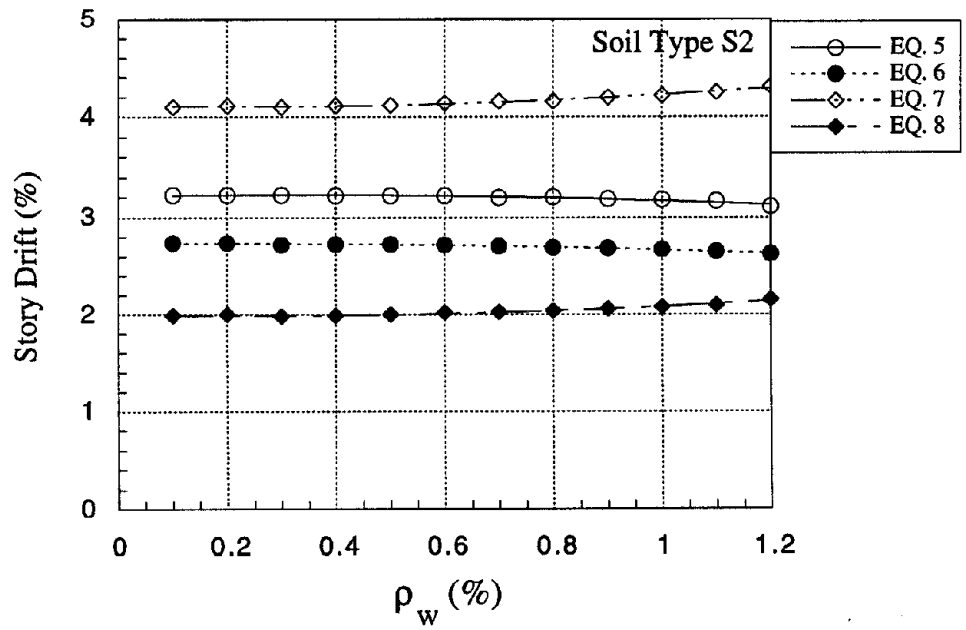

Figure 3.28. Maximum Story Drift, Vary ρ_w, Soil Type 2.

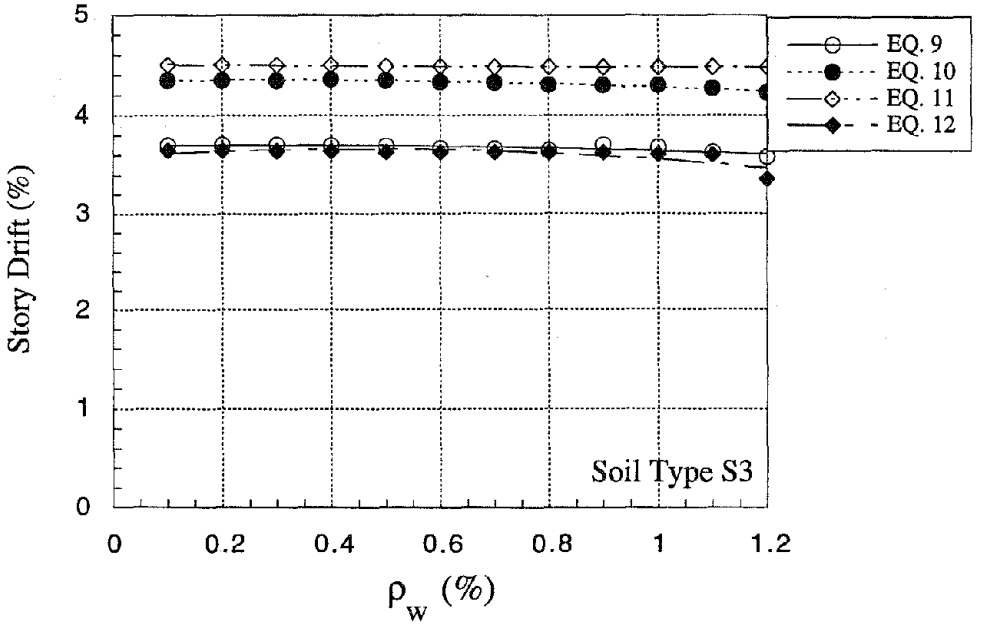

Figure 3.29. Maximum Story Drift, Vary ρ_w, Soil Type 3.

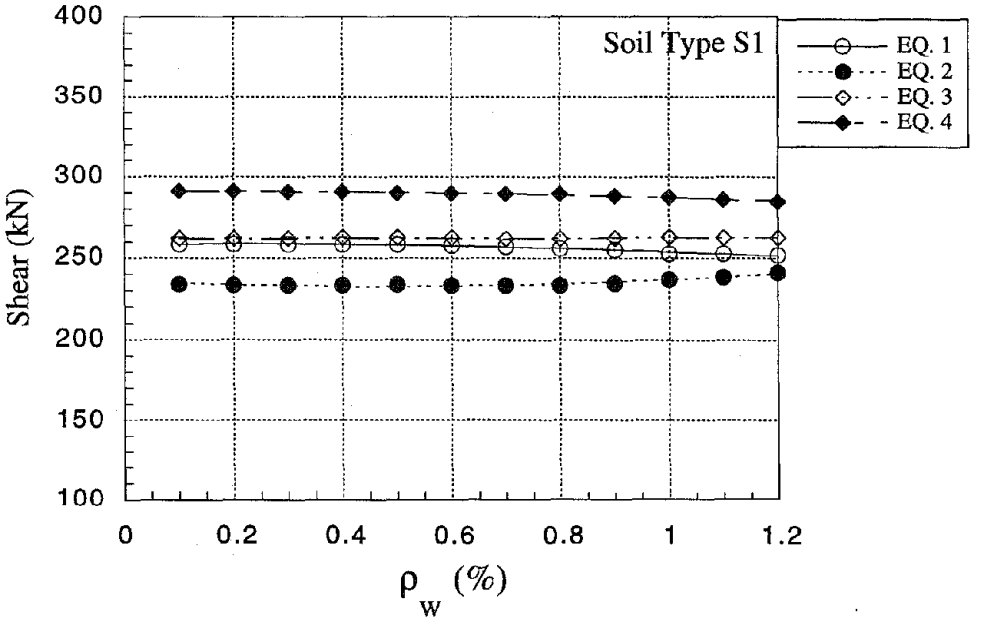

Figure 3.30. Maximum Shear Force, Vary ρ_w, Soil Type 1.

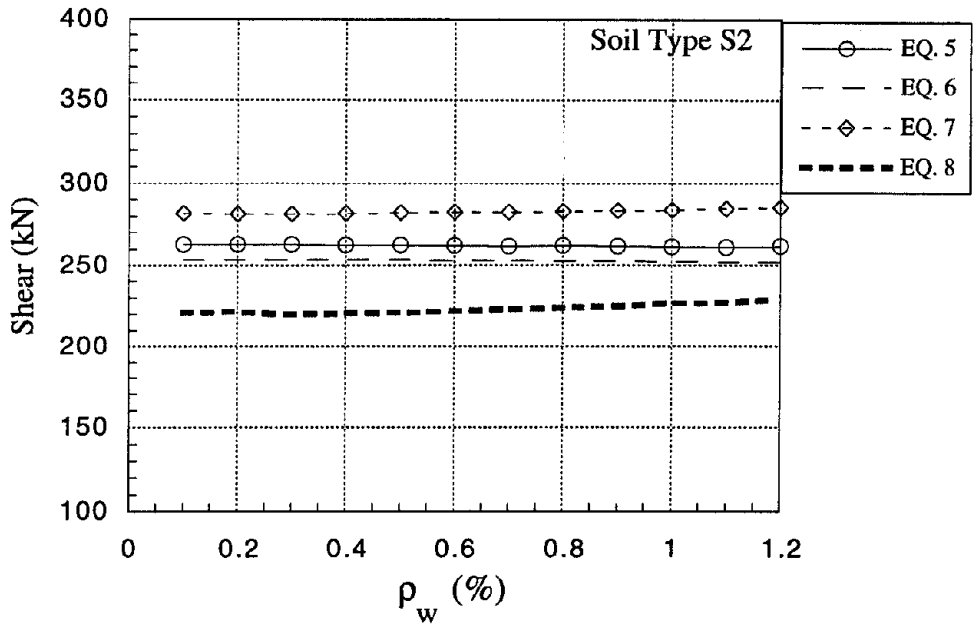

Figure 3.31. Maximum Shear Force, Vary ρ_w, Soil Type 2.

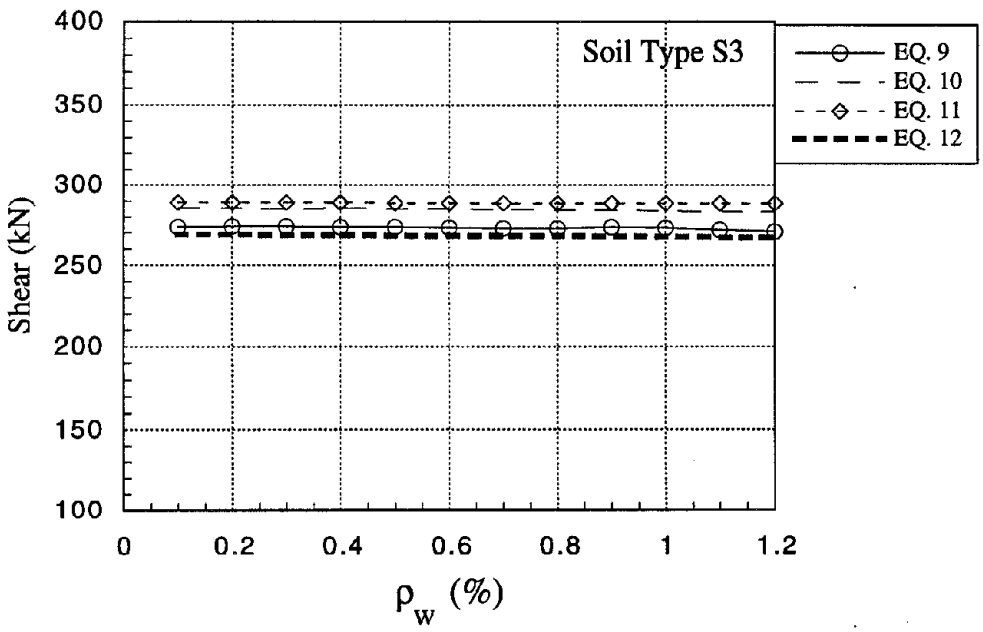

Figure 3.32. Maximum Shear Force, Vary ρ_w, Soil Type 3.

3.5.2.3 CIP Infill Walls, Vary A_c

The trends for both the maximum story drift and shear forces are increased story drifts/shear forces for increasing anchor areas. The maximum drift and shear strength are independent of soil type and record. The story drifts ranged from 2% to 7% and the shear force ranged from 230 kN (51.7 k) to 330 kN (74.2 k). The plots for the maximum drifts and shears are given in Figures 3.33 to 3.38. This was also observed for the quasi-static analysis.

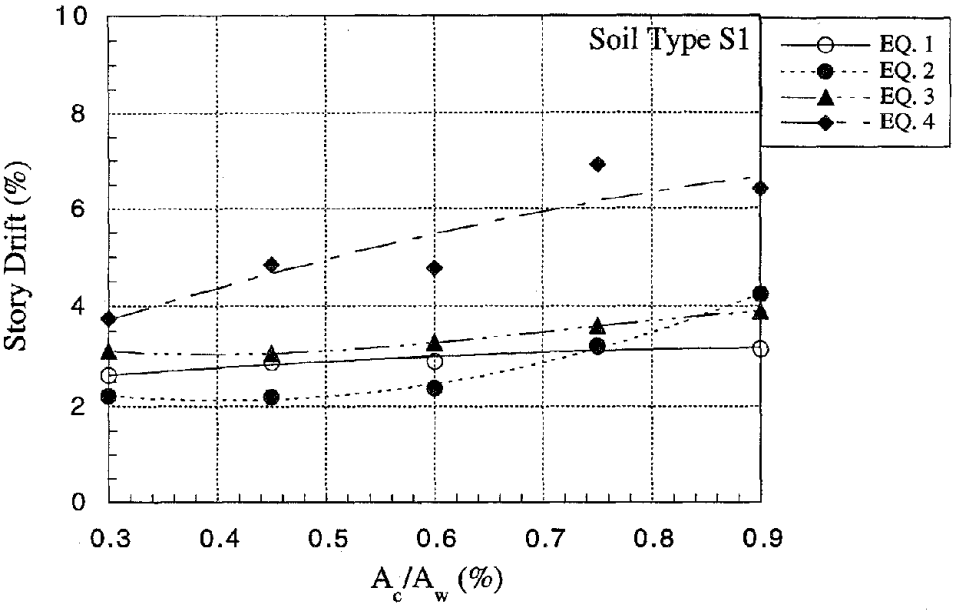

Figure 3.33. Maximum Story Drift, Vary A_c/A_w, Soil Type 1.

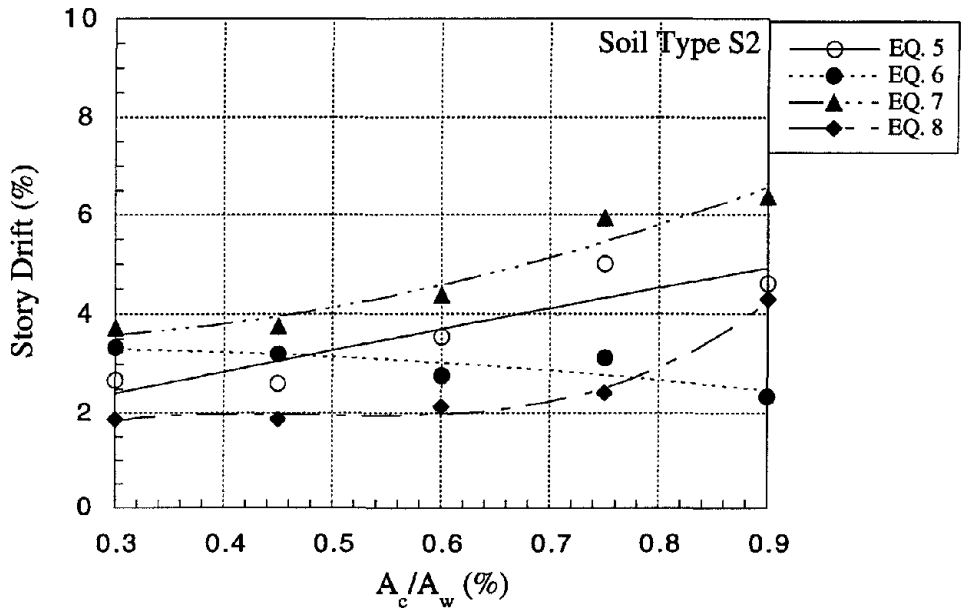

Figure 3.34. Maximum Story Drift, Vary A_c/A_w, Soil Type 2.

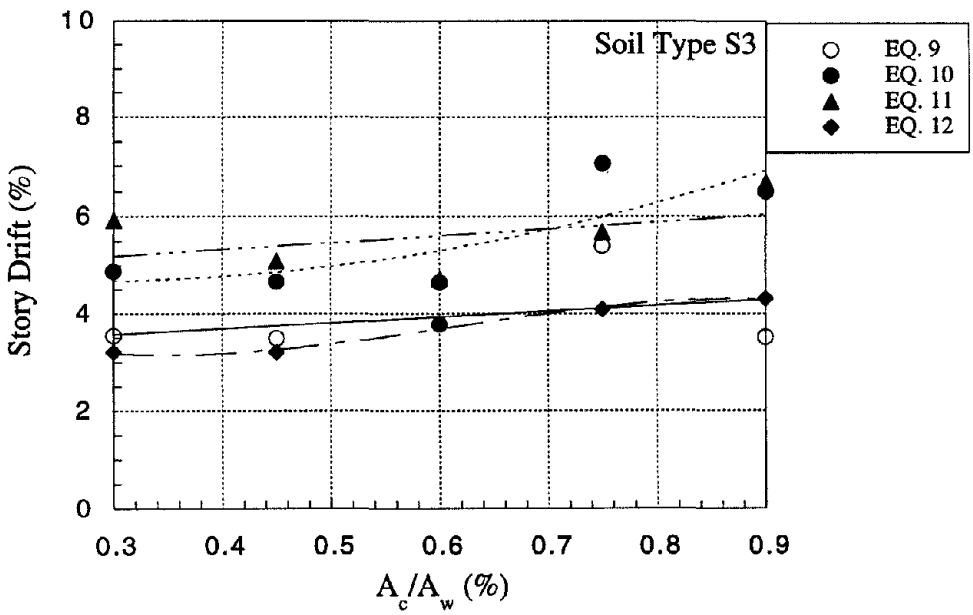

Figure 3.35. Maximum Story Drift, Vary A_c/A_w, Soil Type 3.

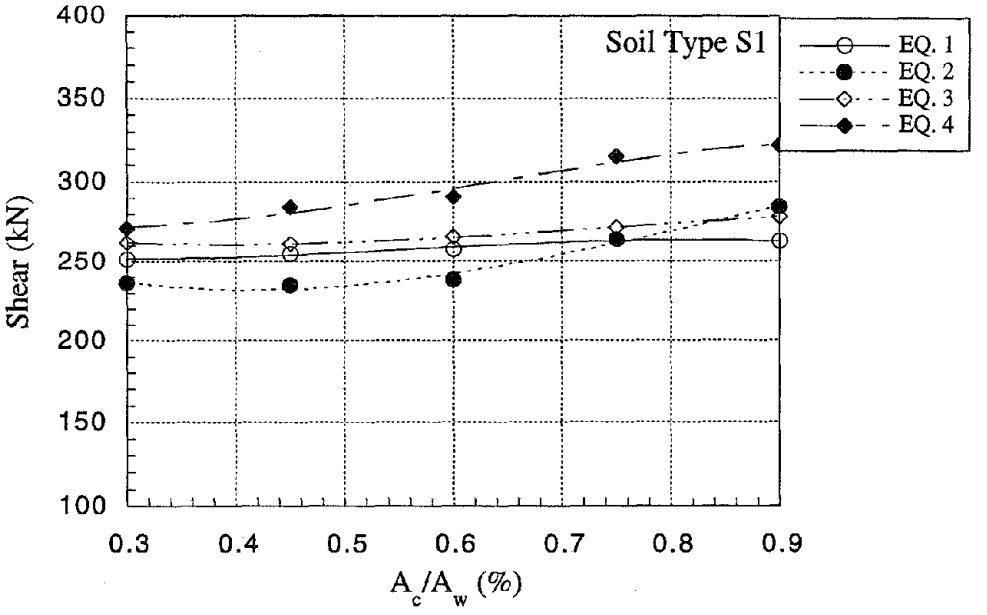

Figure 3.36. Maximum Story Shear, Vary A_c/A_w, Soil Type 1.

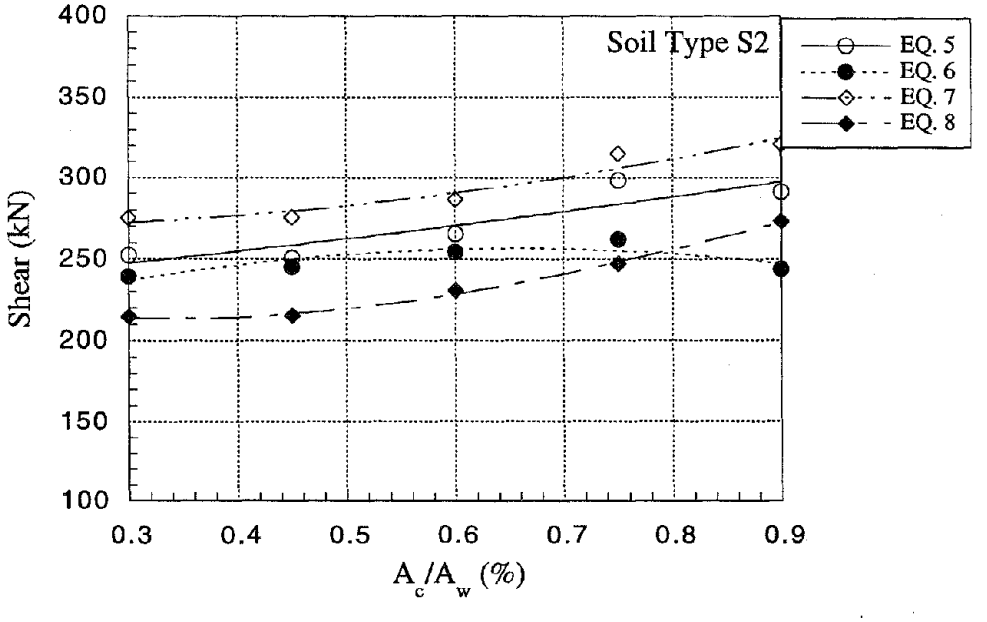

Figure 3.37. Maximum Story Shear, Vary A_c/A_w, Soil Type 2.

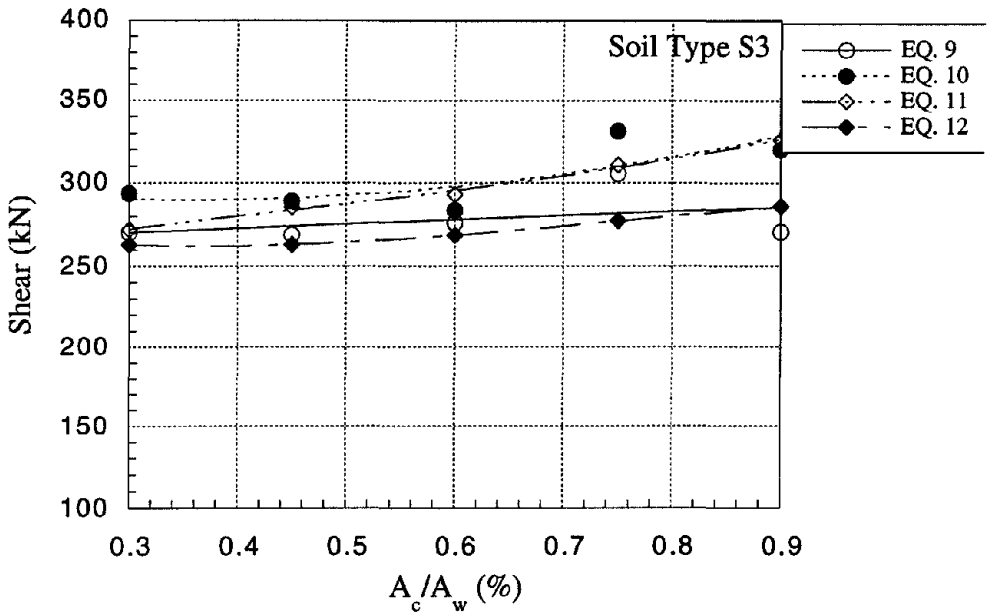

Figure 3.38. Maximum Story Shear, Vary A_c/A_w, Soil Type 3.

3.5.2.4 Precast Infill Walls, Vary ρ_w

As observed in the previous analyses for both precast and CIP infill walls, there was no appreciable increase in the maximum story drift achieved or the maximum shear force obtained for increased values of ρ_w. Again, this trend is independent of soil type and earthquake record. This drift values ranged from 2% to 6% and the shear values ranged from 230 kN (51.7 k) to 290 kN (65.2 k). The plots of the maximum story drifts and shears are given in Figures 3.39 to 3.44.

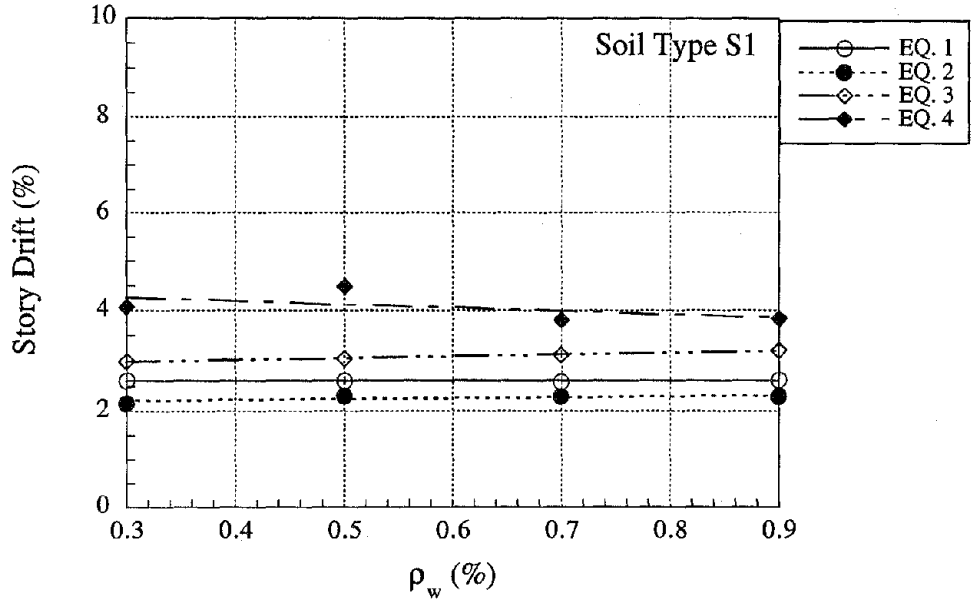

Figure 3.39. Maximum Story Drift, Vary ρ_w, Soil Type 1.

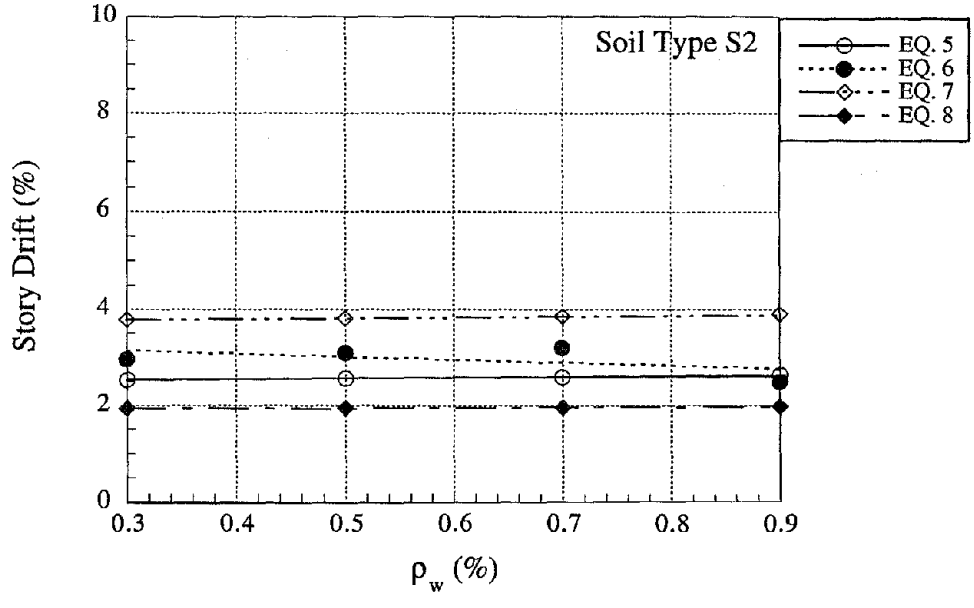

Figure 3.40. Maximum Story Drift, Vary ρ_w, Soil Type 2.

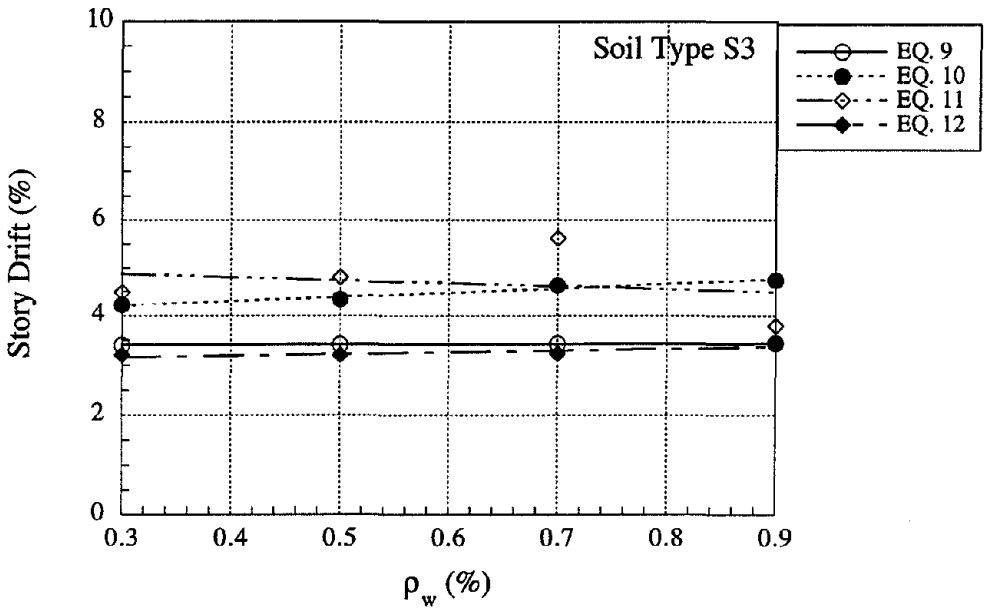

Figure 3.41. Maximum Story Drift, Vary ρ_w, Soil Type 3.

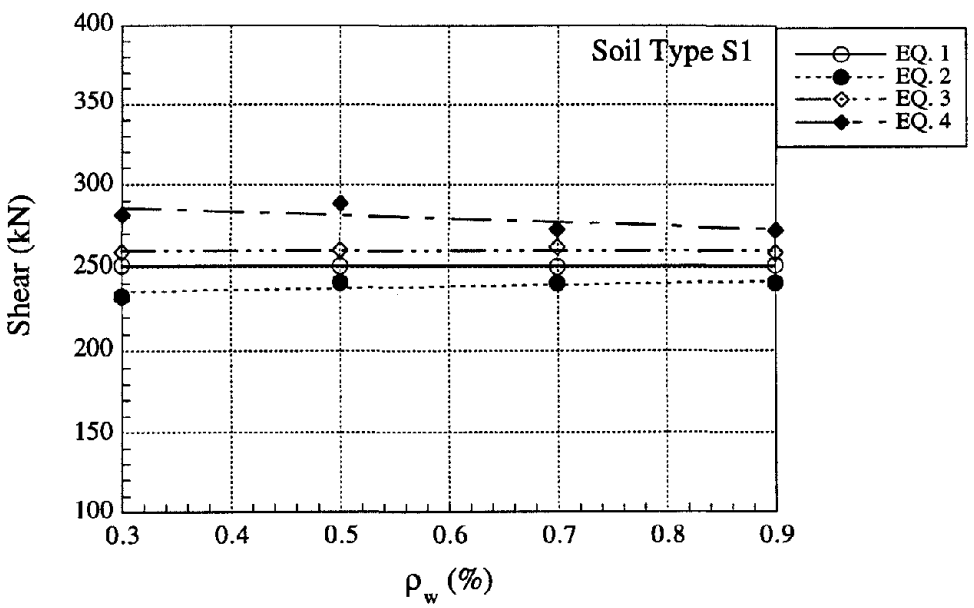

Figure 3.42. Maximum Story Shear, Vary ρ_w, Soil Type 1.

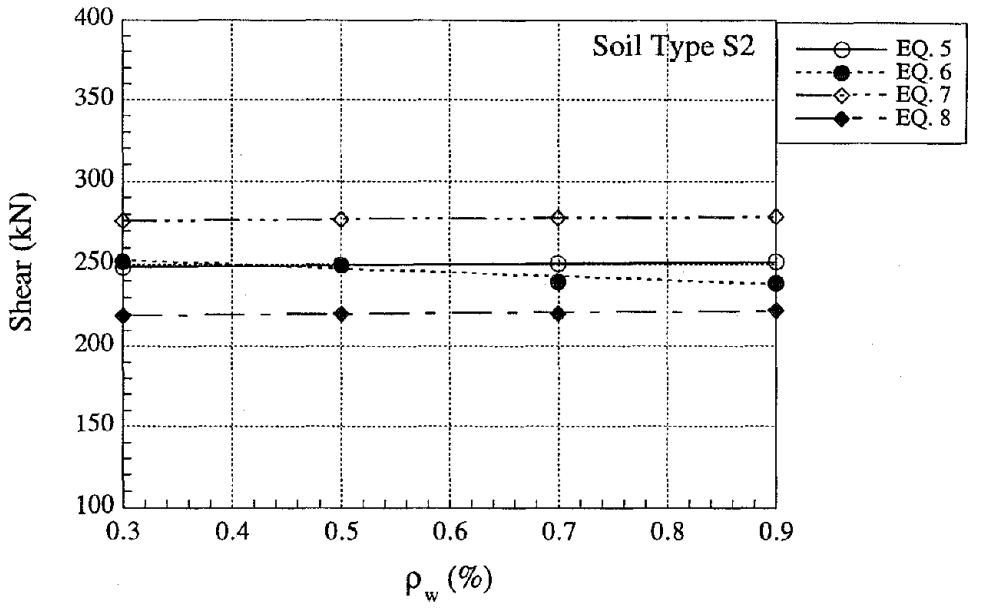

Figure 3.43. Maximum Story Shear, Vary ρ_w, Soil Type 2.

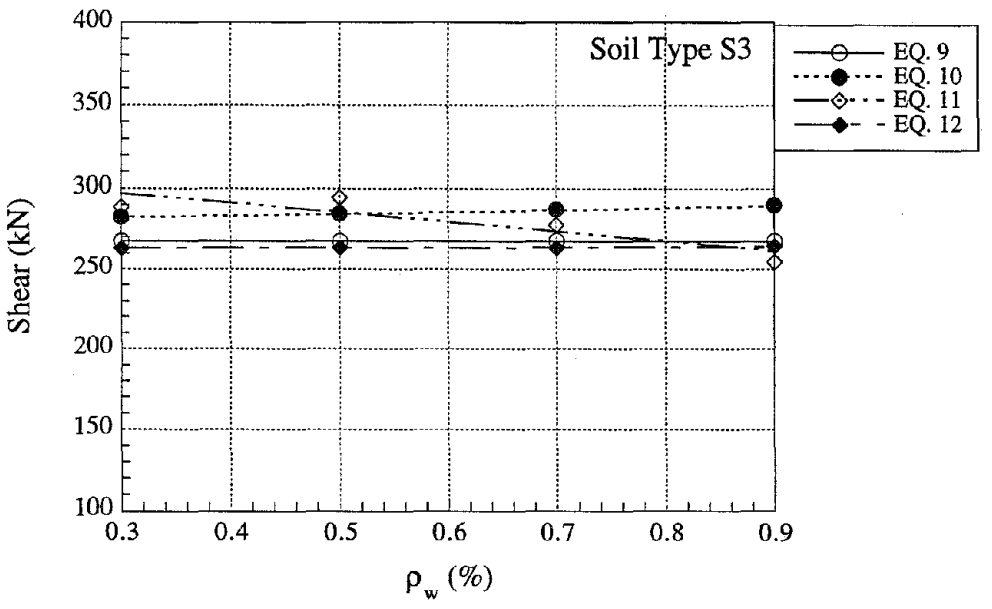

Figure 3.44. Maximum Story Shear, Vary ρ_w, Soil Type 3.

3.5.2.5 Precast Infill Walls, Vary A_c

As seen in Figures 3.45 to 3.47, there are no clear trends for the maximum story drifts for increased ratios of A_c/A_w. The values ranged from 2% to 5%. The maximum shear forces (Figures 3.47 to 3.49) appear to be unchanged for increasing A_c values. They vary from 230 kN (51.7 k) to 300 kN (67.4 k).

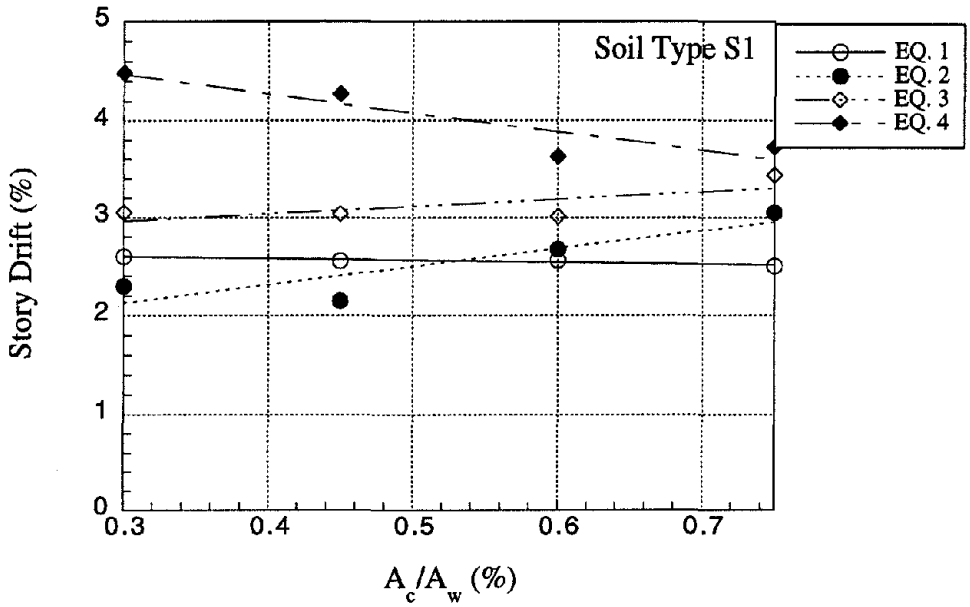

Figure 3.45. Maximum Story Drift, Vary A_c/A_w, Soil Type 1.

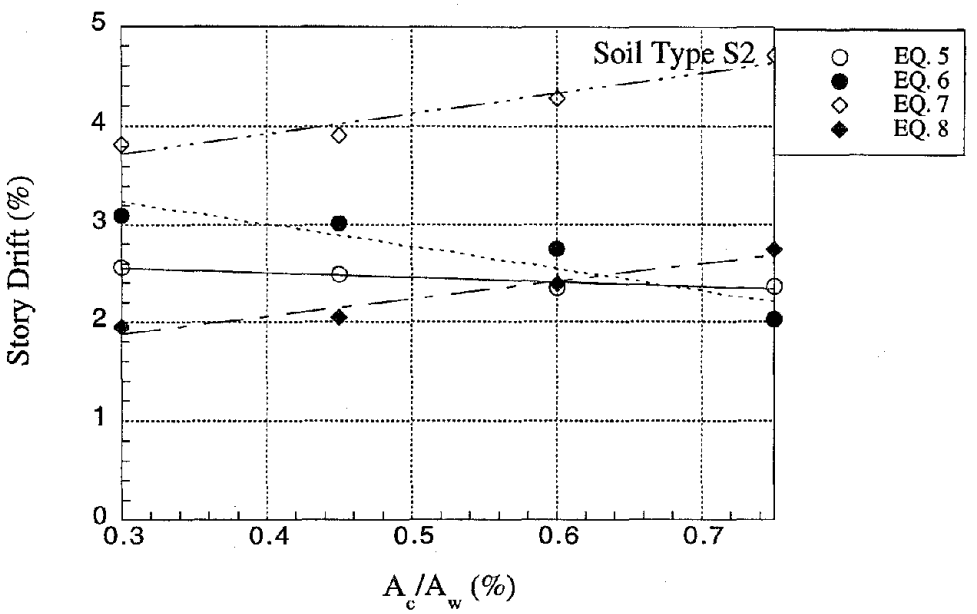

Figure 3.46. Maximum Story Drift, Vary A_c/A_w, Soil Type 2.

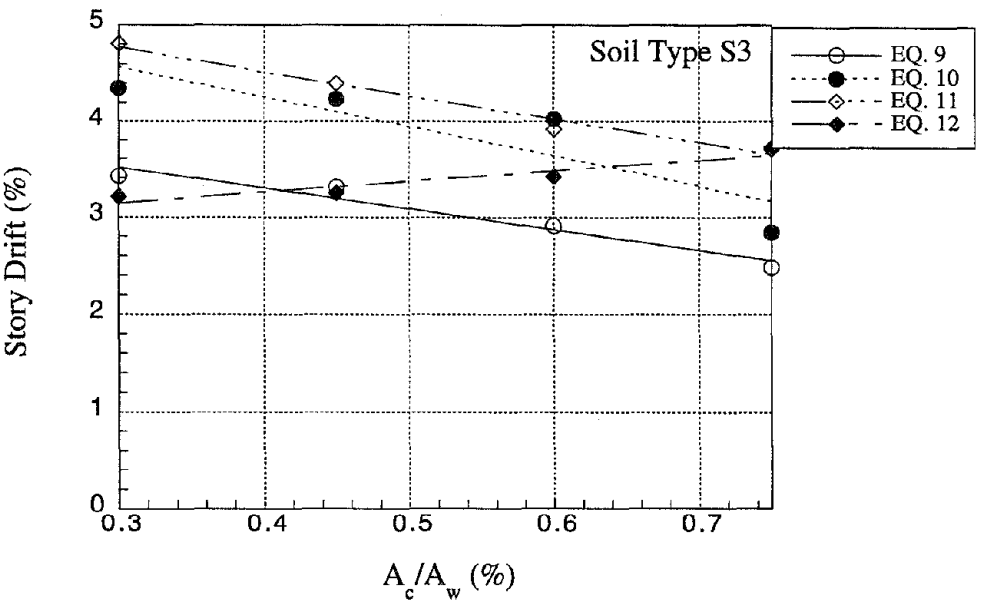

Figure 3.47. Maximum Story Drift, Vary A_c/A_w, Soil Type 3.

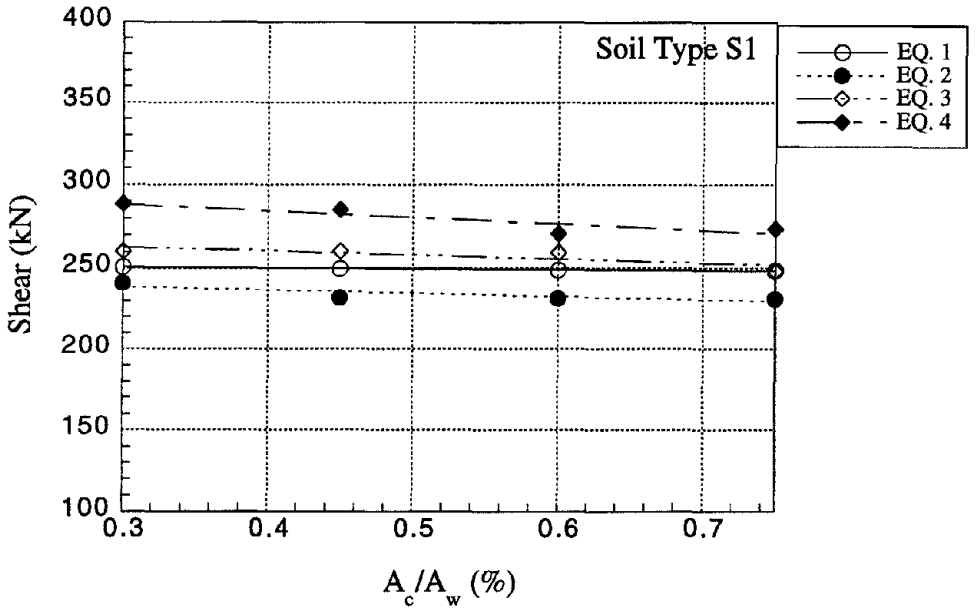

Figure 3.48. Maximum Story Shear, Vary A_c/A_w, Soil Type 1.

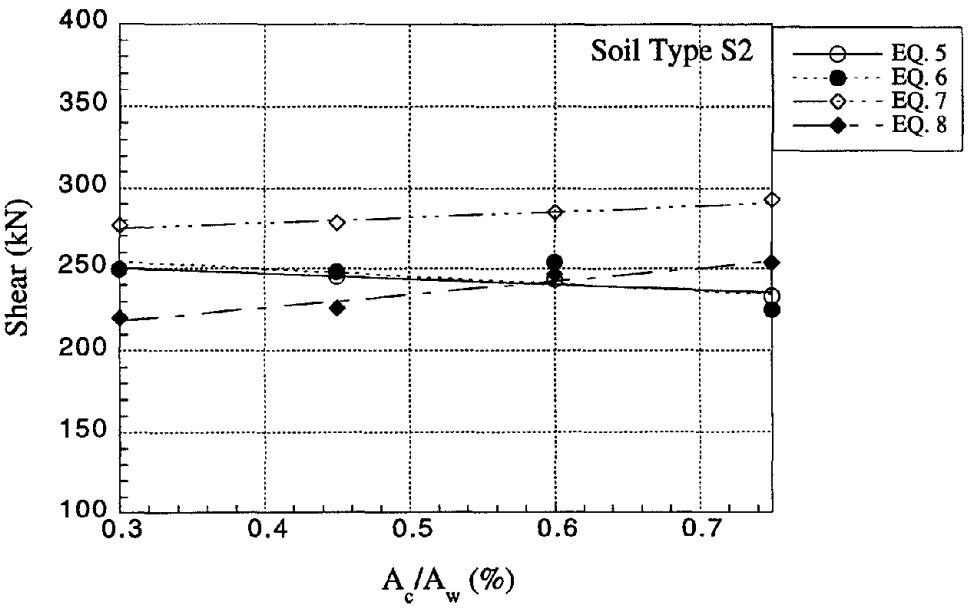

Figure 3.49. Maximum Story Shear, Vary A_c/A_w, Soil Type 2.

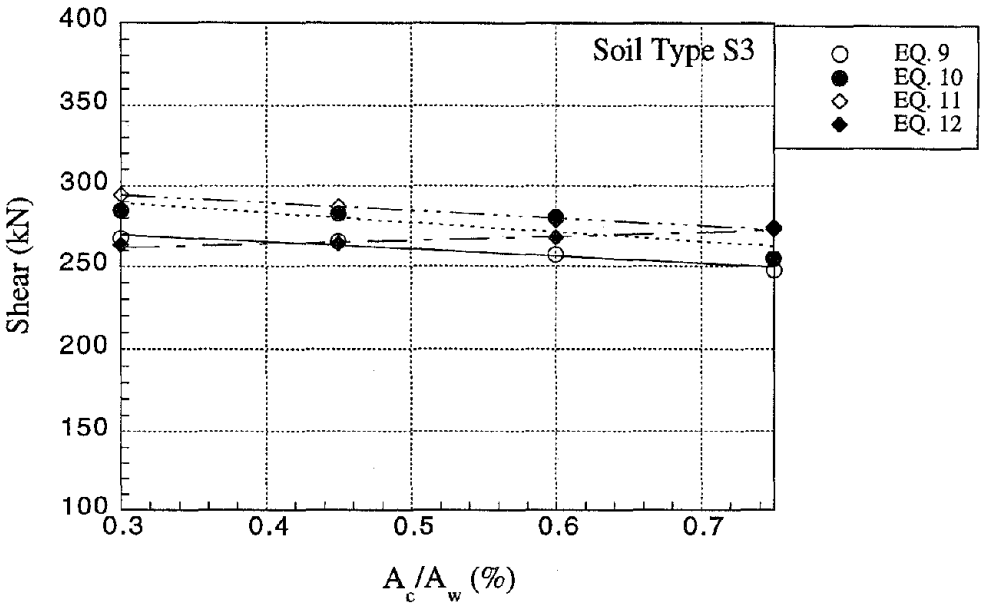

Figure 3.50. Maximum Story Shear, Vary A_c/A_w, Soil Type 3.

4.0 RECOMMENDATIONS FOR GUIDELINES DEVELOPMENT

4.1 GENERAL

The analytical results obtained from the parametric study are used in conjunction with experimental observations extracted from various experimental programs which were systematically reviewed and reported in [Phan, et al, 1993, 1994] for the development of guidelines for seismic strengthening of LRC frame construction by the infill wall techniques. The experimental observations are important because they provide confirmation for analytical results and provide information on design details which are too detailed and complex for the simplified, generic analytical models to capture. These details include the size of anchors used in connecting the infill wall to the LRC frame, the number of rows of anchors, and shear reinforcement for infill walls. The following design guidelines are recommended for consideration in strengthening LRC frames with the infill wall techniques.

The dynamic analyses indicated that the performance of the models did not seem to be affected by the different soil types. Intuitively, one would expect that the softer soils, soil type S3, would increase the ductility demand on a structure. However, since the models analyzed were short and squat with short periods (0.1 s to 0.4 s), the different soil types would have little effect on the ductility demand of the structure. This "insensitivity" to soil type can be seen in the spectral response curves in the UBC [ICBO, 1991] where the spectral accelerations are the same for all three soil types in this period range.

4.2 RECOMMENDED DESIGN GUIDELINES FOR STRENGTHENING WITH INFILL WALLS

- Infill wall thickness, of both CIP and precast infill walls, should be not less than 2/5 the thickness of the bounding column or the top beam of the frame, whichever is smaller, and should not be greater than the thickness of the top beam. This observation was drawn from many experimental programs and confirmed in the parametric study in this report.

- Based on experimental observation, the ratio of the total cross sectional area of the connecting anchors to the area of the infill walls at the wall/frame interface (A_c/A_w) should not be less than 0.8% for successful connection between the infill wall and the existing frame. However, the experiments examined only two ratios, 0.3% and 0.81%. Thus, it is believed that the 0.81% ratio is rather conservative. The parametric study showed a steady increase in both the maximum story drift and shear strength at a ratio of 0.45%, and the increase became less significant for ratios greater than 0.9%. Thus, to be conservative, the number of connecting anchors and their sizes are recommended so that the ratio of A_c/A_w be approximately 0.8% as observed in previous experiments.

- Even though the flexural reinforcement ratio was not a variable in most of the experimental programs, successful infill wall performance was observed in experiments where the reinforcement ratio, in both the vertical and horizontal directions, was greater than or equal to 0.75%.

  The parametric study conducted using the hysteretic models in this study revealed that the infill wall reinforcement ratio did not have an effect on the ultimate performance of the overall infill wall/frame system. However, the ability of the models to predict the influence of flexural reinforcement is limited. This is because the hysteretic models were developed based on results of experiments which did not consider infill wall reinforcement ratio as a variable. For this reason, the infill wall reinforcement ratios, for both the CIP and the precast infill wall techniques and in both vertical and horizontal directions, are recommended to be not less than 0.75%. A shear reinforcement of 0.25 to 1.0% (ratios used successfully in previous experiments) should be provided for confinement of concrete in the infill walls.

The above recommendations were derived from both experimental and analytical observations. Below are recommendations that were extracted from experimental programs conducted by other researchers [see [Phan et. al., (1993) for references]. The effects of these are details could not be easily captured by the hysteretic models.

- Infill walls, either CIP, precast, or shotcrete, should be constructed using concrete with normal range of compressive strength [14 - 50 MPa (2.03 ksi - 7.25 ksi)]. The design compressive strength of the infill wall should be compatible with that of the existing frame.

- If a choice of CIP or precast infill wall is available, the decision should be based on the whether increased strength and stiffness is desired or whether ductility is desired. A CIP infill wall significantly increases the shear strength and stiffness of the frame. A frame with precast infill walls is likely to exhibit only a slight increase in the shear strength, but it would, however, be more ductile than a frame with CIP infill walls.

- Either mechanical wedge anchors or epoxied dowels may be used to connect CIP infill walls to the existing frame. For precast infill walls, only epoxy grouted dowels are recommended. The connectors should be placed, at a minimum, at the interface between the infill walls and top and bottom beams, in predrilled holes on the inner surface of the frame to be strengthened. With respect to the cross section of the infill wall, the connectors should be located at or close to the center line to minimize the eccentricity of the transferred shear force to the infill wall.

- The connector size can be selected based on the above required area of connectors and a connector spacing of not less than 7 D_b and not greater than 30 cm (11.81 in.). D_b is the outside diameter of the connectors.

- When more than one line of connectors is required at the infill wall/frame interface, the distance between the connector lines should be not less than 5 D_b.

- Embedment depth of connectors should be not less than 5 D_b or the thickness of the concrete cover, whichever is greater.

4.3 FUTURE RESEARCH NEEDS

The task undertaken by NIST to develop guidelines for the strengthening of lightly RC frames using the infill wall technique was an attempt to collect and correlate the available data and to present them in a practical format for use by designers. The guidelines and analytical procedures were based on the experimental work conducted by other researchers. However, only a small number of tests were available to date.

As mentioned earlier in the report, the equations for predicting the hysteretic parameters for the infill walls need to be refined. The equations were derived based on 54 experimental tests which were all that were available at the time. From among the 54 tests, there were 93 variables which could possibly have an effect on the computation of the hysteretic parameters. In addition, variables such as different loading history and scale factor cannot easily be quantified and were not taken into account. Therefore, additional experimental tests need to be conducted to add to the existing database - both static and shake table tests. Also, tests of multi-story and multi-bay frames are needed to study the overall behavior of the frame and not just localized behavior. Once these test data are available, the analytical procedure can be expanded to include multi-bay, multi-story bents.

A workshop is planned at NIST (June, 1995) to determine and to prioritize the research needs for the strengthening of lightly RC frames. These recommendations will be used to refine the current research approach and to develop a research plan for improving the seismic performance of lightly reinforced concrete frames at NIST.

REFERENCES

Alcocer, S. M. and Jirsa, J. O. [1990], "Assessment of the Response of Reinforced Concrete Frame Connections Redesigned by Jacketing", Proceedings of Fourth U.S. National Conference on Earthquake Engineering, EERI, Volume 3, pp. 295-304, Palm Springs, California, May.

Aoyama, H., Kato, D., Katsumata, H., Hosokawa, Y. [1984], "Strength and Behavior of Postcast Shear Walls for Strengthening of Existing Reinforced Concrete Buildings" List of Manuscripts Submitted to Eighth WCEE in San Francisco 7/1984, Aoyama Laboratory, Department of Architecture, University of Tokyo, Hongo, Bunkyo-ku, Tokyo 113, Japan.

Aoyama, H. [1986], "Seismic Strengthening of Existing Reinforced Concrete Buildings in Japan", Department of Architecture, Faculty of Engineering, The University of Tokyo, Japan, September.

Aoyama, H. and Shiohara, H. [1986], "Plastic Analysis for Ultimate Strength of Reinforced Concrete Shear Walls", Department of Architecture, Faculty of Engineering, The University of Tokyo, September.

Beres, A., El-Borgi, S., White, R. N., and Gergely, P. [1992a], "Experimental Results of Repaired and Retrofitted Beam-Column Joint Tests in Lightly Reinforced Concrete Frame Buildings", Technical Report NCEER-92-0025, October.

Beres, A., White, R. N., and Gergely, P. [1992b], "Seismic Behavior of Reinforced Concrete Frame Structures with Nonductile Details: Part I - Summary of Experimental Findings of Full Scale Beam-Column Joint Tests", Technical Report NCEER-92-0024, September.

Beres, A., El-Borgi, S., White, R. N., and Gergely, P. [1992c], "Full-Scale Tests of Retrofitted Beam-Column Joints in Lightly Reinforced Concrete Frame Buildings", Internal Report to NIST, School of Civil and Environmental Engineering, Cornell University, Ithaca, New York, March.

Building Seismic Safety Council [1992], "NEHRP Handbook of Techniques for the Seismic Rehabilitation of Existing Buildings", Building Seismic Safety Council of the National Institute of Building Sciences, Program on Improved Seismic Safety Provisions, Washington D.C.

Higashi, Y., Endo, T., Ohkubo, M., and Shimizu, Y. [1980], "Experimental Study on Strengthening Reinforced Concrete Structure by Adding Shear Wall" Proceedings of the Seventh WCEE, Volume 7, p. 173-180, Istanbul, Turkey, September.

Higashi, Y., Endo, T., and Shimizu, Y. [1981], "Experimental Studies on Retrofitting of Reinforced Concrete Structural Members", Proceedings of the Second Seminar on Repair and Retrofit of Structures, pp. 126-155, University of Michigan, Ann Arbor, MI, May.

International Conference of Building Officials [1991], Uniform Building Code, Whittier, CA.

Phan, L. T, Todd, D. R., and Lew, H. S. [1993], "Strengthening Methodology For Lightly Reinforced Concrete Frames - I", NISTIR 5128, National Institute of Standards and Technology, February.

Phan, L. T., Todd, D. R. and Lew, H. S. [1994], "Strengthening Methodology for Lightly Reinforced Concrete Frames - II, Recommended Calculation Techniques for the Design of Infill Walls," NISTIR 5421, National Institute of Standards and Technology, Gaithersburg, MD, 20899, May.

Park, Y. J., Reinhorn, A. M., and Kunnath, S. K. [1987], "IDARC: Inelastic Damage Analysis of Reinforced Concrete Frame-Shear Wall Structures", National Center for Earthquake Engineering Research, Technical Report NCEER-87-0008, July.

Priestley, M. J. N., ed. [1992], Report on the Third U.S. PRESSS Coordinating Meeting, Report No. PRESSS-92/02, Dept. of Applied Mechanics & Engineering Sciences, UCSD, La Jolla, CA, August.

Yunfei, H., Yufeng, C., Chang, S., and Bainian, H. [1986], "The Experimental Study of a Two-Bay Three Story Reinforced Concrete Frame Under Cyclic Loading", Proceedings of the Eighth Symposium on Earthquake Engineering, Roorkee, India.

APPENDIX A: SAMPLE INPUT FILE FOR PROGRAM IDARC

```
1 Bay, 1 Story, CIP INFILLED Frame, tw = 125 mm, rho=0.5
CONTROL DATA
1,1,2,1,0
ELEMENT TYPES
1,1,1,0,0,0
ELEMENT DATA, 2 cols, 1 bms, 1 swalls
2,1,1,0,0,0,0
UNITS SYSTEM: KN - MM
2
FLOOR ELEVATION
1500.0
DESCRIPTION OF IDENTICAL FRAMES
1
PLAN CONFIGURATION: NUMBER OF COLUMN LINES (j=1,3)
3
NODAL WEIGHTS
1,1, 22.24, 22.24, 22.24
CODE FOR SPECIFICATION OF USER PROPERTIES
0
CONCRETE PROPERTIES
1, 0.0402, 0.0, 0.0, 0.0, 0.0, 0.0
2, 0.0402, 0.0, 0.0, 0.0, 0.0, 0.0
REINFORCEMENT PROPERTIES
1, 0.4, 0.0, 0.0, 0.0, 0.0
HYSTERETIC MODELING RULES
1
1, 24.54, 0.00, 0.70, 0.45
MOMENT CURVATURE ENVELOPE GENERATION
1
COLUMN DIMENSIONS
1, 1498.6,149.86,149.86
  1, 1.17188e+10, 897.97, 400.0, 34975.1, 67307.5, 0.000349, 0.00126, 3.01e+7,
                          34975.1, 67307.5, 0.000349, 0.00126, 3.01e+7
  1, 1.17188e+10, 897.97, 400.0, 34975.1, 67307.5, 0.000349, 0.00126, 3.01e+7,
                          34975.1, 67307.5, 0.000349, 0.00126, 3.01e+7
BEAM MOMENT CURVATURE ENVELOPE GENERATION
1
BEAM DIMENSIONS
1,3000.0,125.0,125.0
   1, 1.5755e+10, 400.0, 11298.5, 33895.4, 0.000207, 0.00573, 3.558e+7,
                         11298.5, 33895.4, 0.000207, 0.00573, 3.558e+7
   1, 1.5755e+10, 400.0, 11298.5, 33895.4, 0.000207, 0.00573, 3.558e+7,
```

11298.5, 33895.4, 0.000207, 0.00573, 3.558e+7
SHEAR WALLS MOMENT CURVATURE ENVELOPE GENERATION
1
SHEAR WALL DIMENSIONS
1, 2750.0, 4897.6
1, 4.63e+11, 2.3597e+05, 5.0209e+05, 1.99e-05, 0.000597, 6.39e+8
2.3597e+05, 5.0209e+05, 1.99e-05, 0.000597, 6.39e+8
1, 4.63e+11, 2.3597e+05, 5.0209e+05, 1.99e-05, 0.000597, 6.39e+8
2.3597e+05, 5.0209e+05, 1.99e-05, 0.000597, 6.39e+8
1,2.2e6,1879.0,1921.0,0.002,0.004,1650.0,1879.0,1921.0,0.002,0.004,1650.0
COLUMN CONNECTIVITY
1,1,1,1,0,1
2,1,1,3,0,1
BEAM CONNECTIVITY
1,1,1,1,1,3
SHEARWALL CONNECTIVITY
1,1,1,2,0,1
ANALYSIS TYPE
3
Long Term Loads
0, 0, 0, 0
Dynamic Analysis
3.0, 0.0, 0.002, 20.0, 2.0
Input Wave (Page A-31) 0=vert. comp. not incl, # acc rec, time interval of input
0, 3939,0.010
Earthquake Acc. file name incl. ext
/usr/people/gcheok/idarc/nceer_eq_rec/designeq/zz12.dat
OUTPUT CONTROL
1,0.02,1
1cipst1_125zz12.prn
MISCELLANEOUS OUTPUT INFORMATION
0,0,0,0